Chapter 4

Phase II

The Phase I observations were the beginning of the program to determine the number of active stars in old open clusters. Different observing strategies were employed in Phase I to determine the optimal observations to make to enable me to detect stellar activity in some of the stars. The stars will be considered active if the brightness changes are significant compared to the photometric errors and if the brightness changes are correlated between different colors observed on the same nights.

The second phase of the observing program began in December 2001 and extended through March 2003. The combination of Phase I and Phase II yielded 235 successful nights, 26,549 individual images, and 5.2×10^6 individual magnitude measurements. Phase II was conducted entirely with the Perkins telescope and the Loral2 CCD. We observed through the BVR filters for all nights, and an attempt was made to place the stars on the same pixels of the CCD from night to night. Only sky flat fields were utilized for the pixel-to-pixel calibration. The observing log is listed in Table 4.1. The B and V data from December 2001 were used also in the Phase I analysis.

The data reduction followed the same procedure as outlined in section 3.2: basic reductions using IRAF, photometry performed by SPS, astrometric transformation to a common coordinate system, photometric transformation by *magmap*, and finally ensemble

Dates (UT)	Usable Nights	Objects
2001 Dec 16-22	3	1, 3, 4
2002 Feb 15-19	3	3
2002 Mar 15-21	4	3
2002 Jul 12-14	0	...
2002 Aug 12 (Q)	1	2
2002 Sep 12-23	11	1, 2, 4
2002 Sep 24 (Q)	1	2
2002 Sep 30 (Q)	1	2
2002 Oct 5 (Q)	1	2
2002 Oct 10-17	7	1, 2, 3, 4
2002 Oct 22 (Q)	1	1
2002 Nov 6-12	4	1, 2, 3, 4
2002 Dec 7-12	5	1, 3, 4
2003 Jan 7-12	3	3, 4
2003 Jan 14 (Q)	1	3, 4
2003 Jan 31 - Feb 6	7	3
2003 Mar 12-15	3	3

Table 4.1: Phase II Observations. All observations taken through the Perkins telescope with the "Loral2" CCD. The BVR filters were used for all runs. A "Q" after the date denotes observations made by the BU Queue observer, as explained in Phase I. The clusters are assigned numbers in order of age: 1 – NGC 7789, 2 – NGC 6819, 3 – M67, 4 – NGC 188.

photometry performed by *diffmag*. The parameters used for each program were the same. For each cluster, the data through each of the B, V, and R filters were reduced.

4.1 Observations

4.1.1 NGC 7789

NGC 7789 was observed on 23 nights from December 2001 to December 2002. Since the data from three filters were used, a check file of median differential magnitudes was produced by *diffmag* for each filter. The check files are plotted in Figure 4.1. The frames are numbered sequentially in each filter; since we cycled through the filters, the frame numbers roughly match between filters. Indeed, similar features can be seen in each plot, such as the bump around frame 350. None of the data deviated far enough from the others

to be rejected.

4.1.2 NGC 6819

NGC 6819 was observed on sixteen nights from August to December 2002; this cluster was observed the least during Phase II. The photometry check files are plotted in Figure 4.1.

4.1.3 M67

M67 was observed on 36 nights from December 2001 to March 2003; this cluster was observed the most during Phase II. The photometry check files are plotted in Figure 4.1. Many more frames were taken of M67 than the other clusters because it was observed the most nights and because the exposure times were shorter than for the other clusters.

4.1.4 NGC 188

NGC 188 was observed on 21 nights from December 2001 to January 2003. The photometry check files are plotted in Figure 4.1.

4.1.5 Photometric Errors

The photometric errors for each of the filters are evaluated in the same fashion as Phase I. σ_{phot} is compared to σ_f to see how well SPS and *diffmag* are estimating the photometric errors. Also compared are σ_{rms} and σ_{mean}, recalling that σ_{rms} is the RMS value of the nightly mean differential magnitudes, and σ_{mean} is the RMS of the standard deviations of the mean of the nightly mean differential magnitudes. The ratio σ_f/σ_{phot} should be unity if SPS is adequately estimating the photometric errors. The ratio $\sigma_{rms}/\sigma_{mean}$ should also be unity for a non-variable star. Figure 4.2 plots the two ratios in half or full magnitude bins for all four clusters. Since fewer stars were observed in the Phase II data, fewer stars fall in each bin, causing the binned ratios to vary less smoothly with magnitude.

Taking NGC 7789 as an example, the figure shows that SPS and *diffmag* overestimate

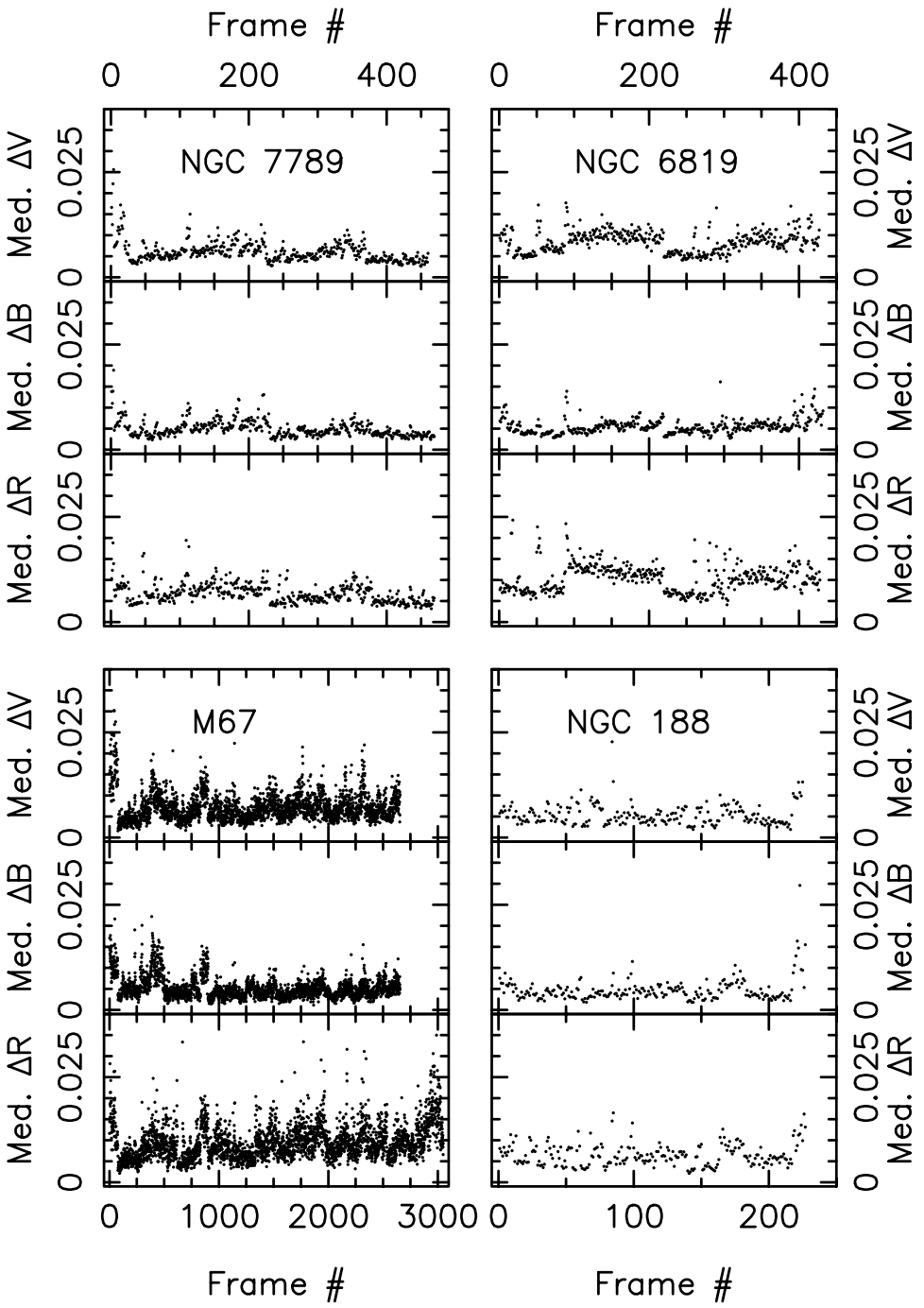

Figure 4.1: Differential ensemble photometry check. The x-axis numbers the B, V, and R frames, independently, for the observations in the indicated clusters. The y-axis is the median differential magnitude for each frame. Many more images were taken of M67 because the exposure times were shorter, since the cluster is so bright.

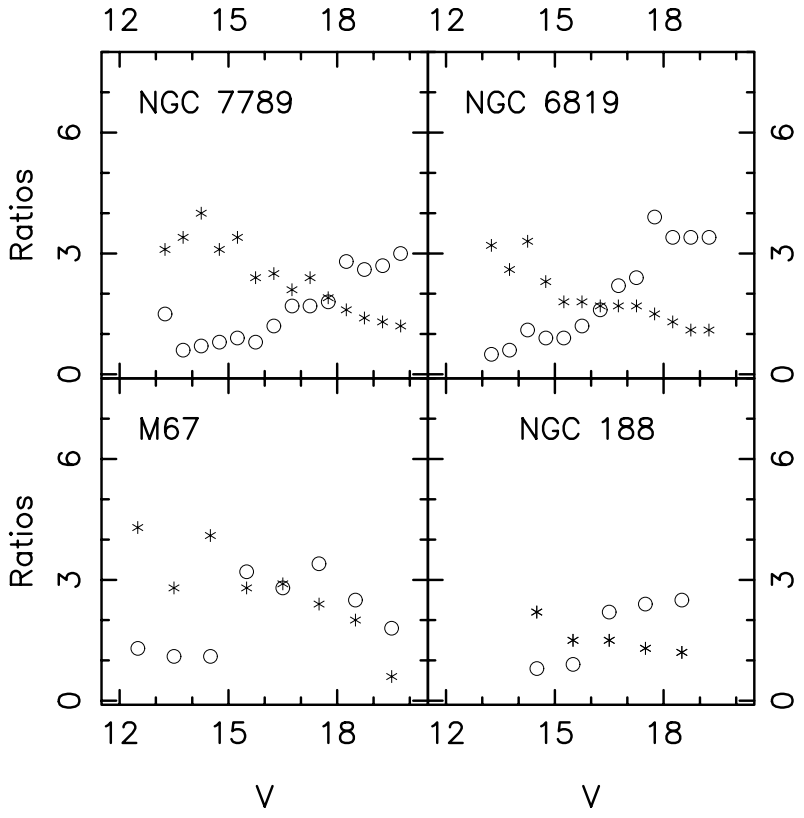

Figure 4.2: Plot of the ratios σ_f/σ_{phot} (circles) and $\sigma_{rms}/\sigma_{mean}$ (asterisks) for the clusters indicated.

the photometric errors in the range 13.5 < V < 16, since the ratio of σ_f/σ_{phot} is less than one. After V=16, the ratio climbs to nearly three, showing that for faint stars, SPS does not estimate the errors as well. This overestimation and underestimation are more severe for the stars in each cluster in the Phase II data compared to the Phase I data (Figure 3.30). It is not clear whether this is due to photometric noise that increases with magnitude or the intrinsic variability of the fainter stars.

The figure also shows that the ratio $\sigma_{rms}/\sigma_{mean}$ declines sharply with magnitude. Figure 4.3 shows the constituents of this ratio for each cluster. Again using NGC 7789 as an example, the plot shows that σ_{rms} is approximately 2.5 mmag brighter than σ_{mean} for stars 13.5 < V < 15. Assuming that stars in this range are not variable, σ_{rms} should equal σ_{mean}. Thus I have determined an ensemble error (as in Phase I) of 2.5 mmag for the V data in the Phase II dataset for NGC 7789. Using a similar analysis, the ensemble

error for NGC 6819 is 1.5 mmag, for M67 2 mmag, and for NGC 188 1.5 mmag. All of these ensemble errors are smaller than in the Phase I data.

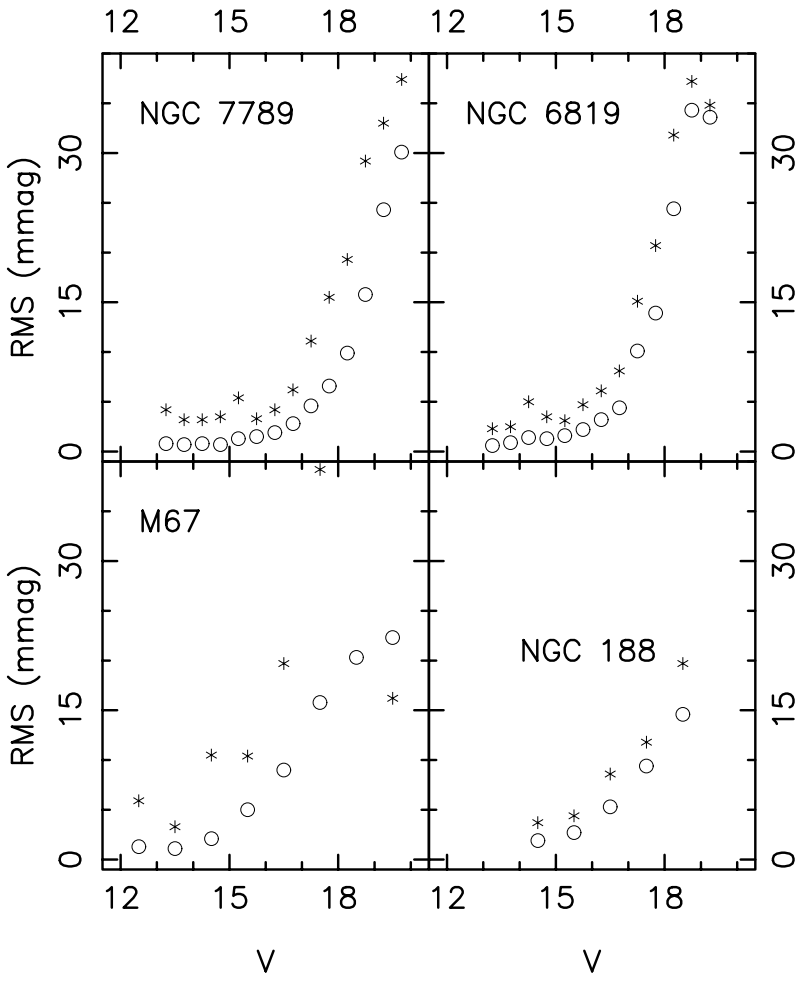

Figure 4.3: Plot of σ_{rms} (asterisks) and σ_{mean} (circles) for the V data for all clusters. The offset between σ_{rms} and σ_{mean} for the bright stars is attributed to the ensemble error.

4.2 Activity on the Nightly Timescale

4.2.1 The Activity Determination

Now I will apply the activity index I developed in Phase I to the V nightly mean differential magnitudes taken in Phase II. Recall that the activity index, A_v, which is described in Equation 3.13, is the RMS amplitude of the brightness fluctuations. The RMS error of

the activity index is σ_{A_v}, described in Equation 3.14. The ratio of these two quantities is the significance index, α_v, shown in Equation 3.15. As before, any star with $\alpha_v \geq 3$ is deemed a candidate variable star.

I calculate the activity index, RMS error, and significance index for all stars falling on the photometric main sequence as determined in Phase I, applying the calculation to the main sequence stars in each cluster. The left column of Figure 4.4 shows the main sequence stars observed for at least five nights through the V filter for all clusters. Significantly fewer main sequence stars were observed in Phase II due to the 3 arcmin field of view of the Loral2 CCD.

I can now apply the significance index calculation. Figure 4.5 shows how α_v varies with magnitude for all of the main sequence stars in each cluster. A typical star in M67 has $\alpha_v \approx 3$; the median significance indices for the other clusters is generally between one and two. Figure 4.6 shows the variation of the median values of A_v and σ_v for the main sequence stars in each cluster.

Following the procedure from Phase I, the next step is to look at the correlation between fluctuations in different colors. I will only deem a star "variable" if it has $\alpha_v \geq 3$ and fluctuations in different colors are correlated at a 99% significant level. I have calculated the linear correlation coefficient r for the stars that have at least five nights with observations in B and V and/or V and R; a night where B, V, and R were observed would count as two nights. Figure 4.7 shows the variation of r with magnitude for the main sequence stars matched in each cluster. Most of the main sequence stars in the three younger clusters are positively correlated; the main sequence stars in NGC 188 show no significant positive correlation. Figure 4.8 shows the correlation coefficient plotted by magnitude for the candidate variables (main sequence stars with $\alpha_v \geq 3$) in each cluster. In the three younger clusters, most candidate variables are positively correlated. The three candidate variables in NGC 188 showed no correlation between the colors.

Table 4.2 summarizes the activity tests for each of the clusters. In NGC 7789, 12% of

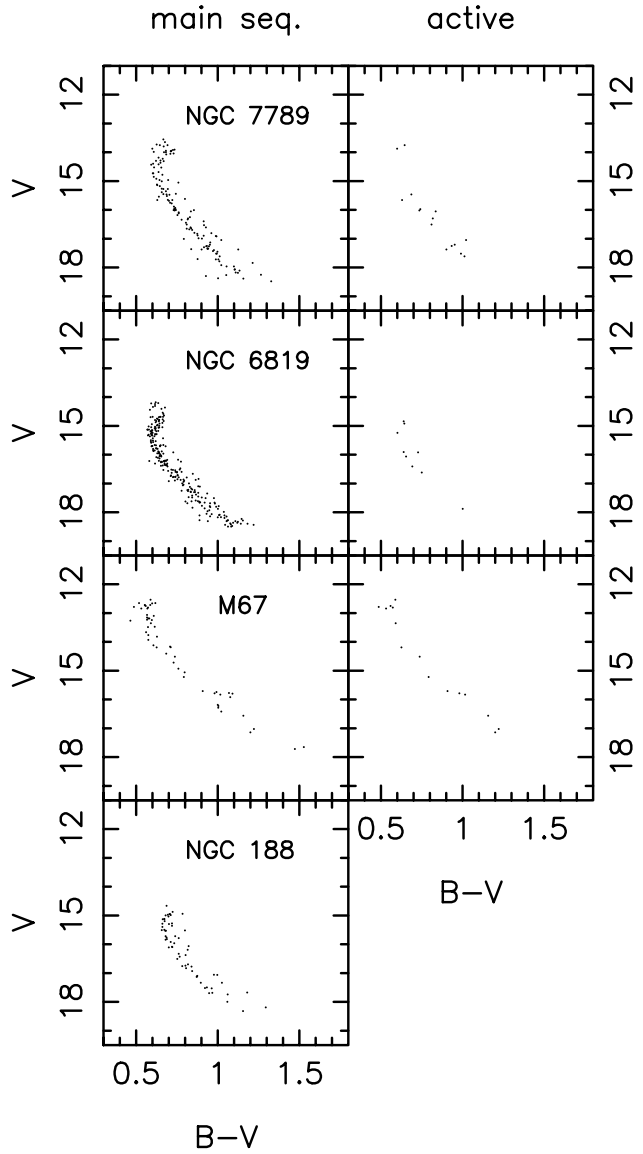

Figure 4.4: Color-magnitude diagrams for each cluster. The left column of panels shows the main sequence stars observed on at least five nights through the V filter for each cluster. The right column of panels shows the stars found to be active in each cluster.

the main sequence stars are active. In NGC 6819, 4% are active; 28% are active in M67, and no main sequence stars are active in NGC 188.

Next I look at how the mean B and R differential magnitudes vary with the mean V differential magnitudes on the same nights. Since the data are less noisy that those in Phase I, a difference is apparent in the B and R data, so they are plotted separately.

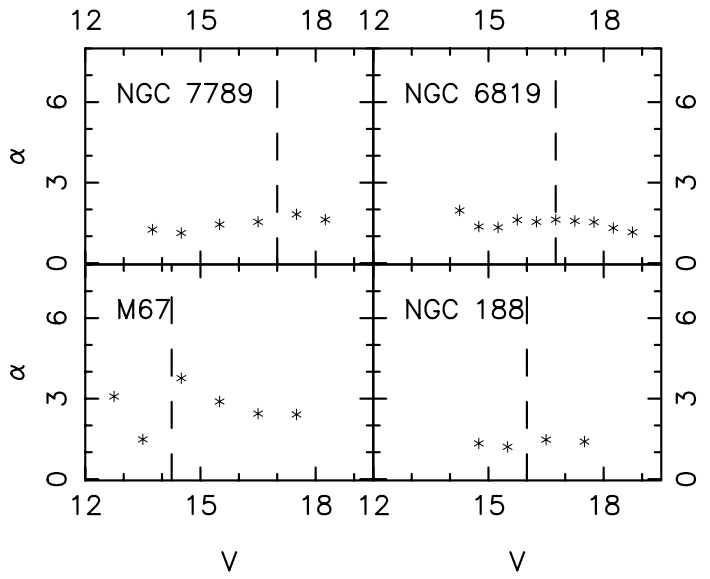

Figure 4.5: The significance index (α_v) as a function of magnitude for the main sequence stars in the indicated clusters. The typical main sequence star has an activity index between one and two, except in M67, where the significance indices are generally higher. There are few stars in each magnitude bin, especially in M67 and NGC 188. The vertical dashed line is the approximate magnitude of the Sun at the distance of each cluster.

Cluster	σ_{ens}	# MS	# Cand. Var.	# MS	# 99% sig.	# Active
NGC 7789	2.5	136	20 (15%)	136	99 (73%)	16 ± 4 (12%)
NGC 6819	1.5	251	12 (5%)	251	133 (53%)	9 ± 3 (4%)
M67	2.0	53	21 (40%)	53	42 (79%)	15 ± 4 (28%)
NGC 188	1.5	62	3 (5%)	62	23 (37%)	0

Table 4.2: Summary of Activity for Phase II. The second column lists the ensemble errors in millimagnitudes that were determined from the plots of σ_{mean} and σ_{rms}. The third column lists the number of main sequence stars with at least five nights of observations in V that were included in the activity index calculation. The fourth column is the number of candidate variable stars found. The fifth column is the number of main sequence stars with at least five pairs of B and V and/or V and R observations on the same night; these stars were included in the correlation coefficient calculation. The sixth column is the number of stars whose correlation coefficients were 99% significant; the uncertainty is just the square root.

Figure 4.9 shows the mean V magnitudes versus the mean B magnitudes for the main sequence stars in the left column of panels for each cluster; the right column of panels shows the mean V magnitudes versus the mean R magnitudes. The main sequence stars

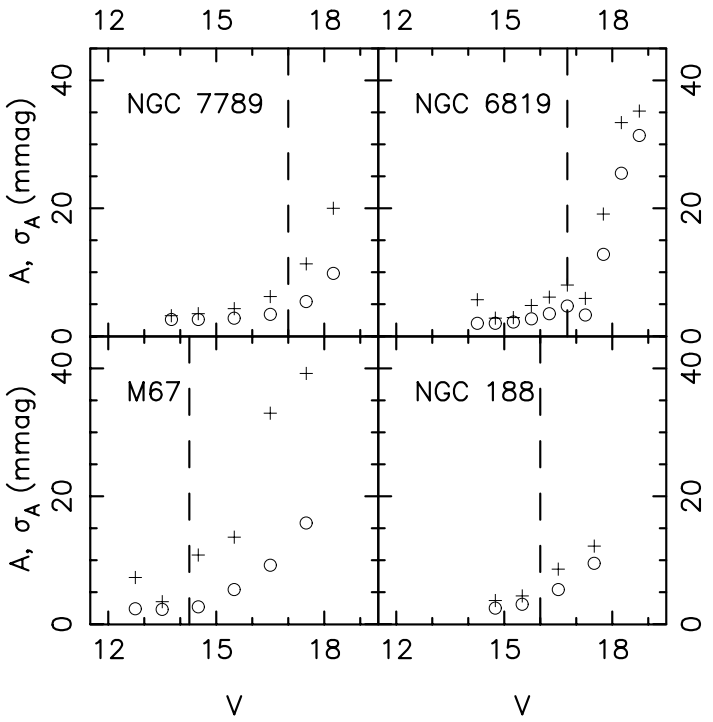

Figure 4.6: The activity index (A_v, crosses) and its error (σ_{A_v}, circles) as a function of magnitude for the indicated clusters. For M67 and NGC 188, few stars are in each magnitude bin. The vertical dashed line is the approximate magnitude of the Sun at the distance of each cluster.

show a distinct positive correlation in the three younger clusters. The stars in NGC 188 show a only a hint of a positive correlation. Figure 4.10 shows the same type of plot for the active stars in each cluster. The correlation between the colors in these plots is strong enough to show that the ΔV vs. ΔB and ΔV vs. ΔR correlations have different slopes.

For both Figures 4.9 and 4.10, lines have been fit to the data using the method of least squares. The slopes and other fit results are listed in Table 4.3. The slopes are similar within each cluster. Using the method of least squares to fit the lines technically violates one of the principals of least squares: the uncertainties in the x-direction should be much less than those in the y-direction. In this case, the uncertainties in each direction are of the same order.

Compared to the Phase I data in Figure 3.17, the random scatter in Figure 4.10 is significantly less and the correlation can be seen at a much lower amplitude. This strong

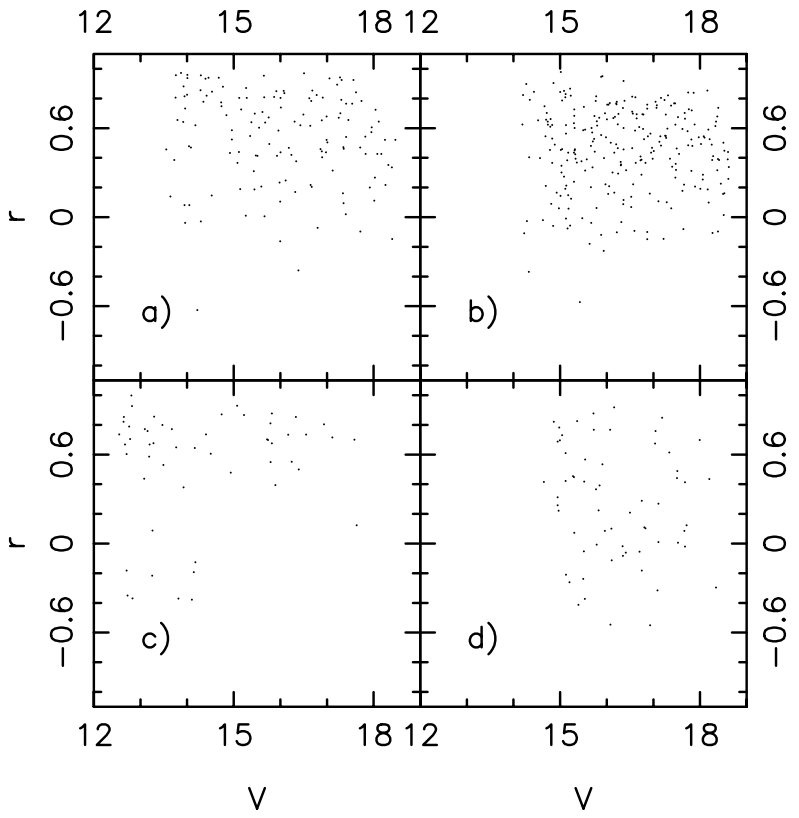

Figure 4.7: The correlation coefficient (r) as a function of magnitude for all main sequence stars in all clusters studied. Panel a is for NGC 7789, b is for NGC 6819, c is for M67, and d is for NGC 188. The stars in the first three clusters show a tendency to be positively correlated, but that tendency is much weaker in NGC 188.

correlation would be expected of brightness changes due to stellar activity. I designate these stars as "active".

Although the majority of the main sequence stars are not classified as active, the ensemble of stars in the three younger clusters clearly show a positive correlation between observations in different colors (Figure 4.9). How can this level of activity be quantified? Since any true brightness fluctuations caused by thermal processes on the star must be positively correlated, any fluctuations perpendicular to the correlation must be purely instrumental. Along the direction of the correlation, the fluctuations are caused by a combination of noise and real variability, which is what I want to quantify.

Assuming that the noise and variability distributions are Gaussian in form, I could fit Gaussians to the plots and find the full widths at half-maximum of the Gaussians. (This

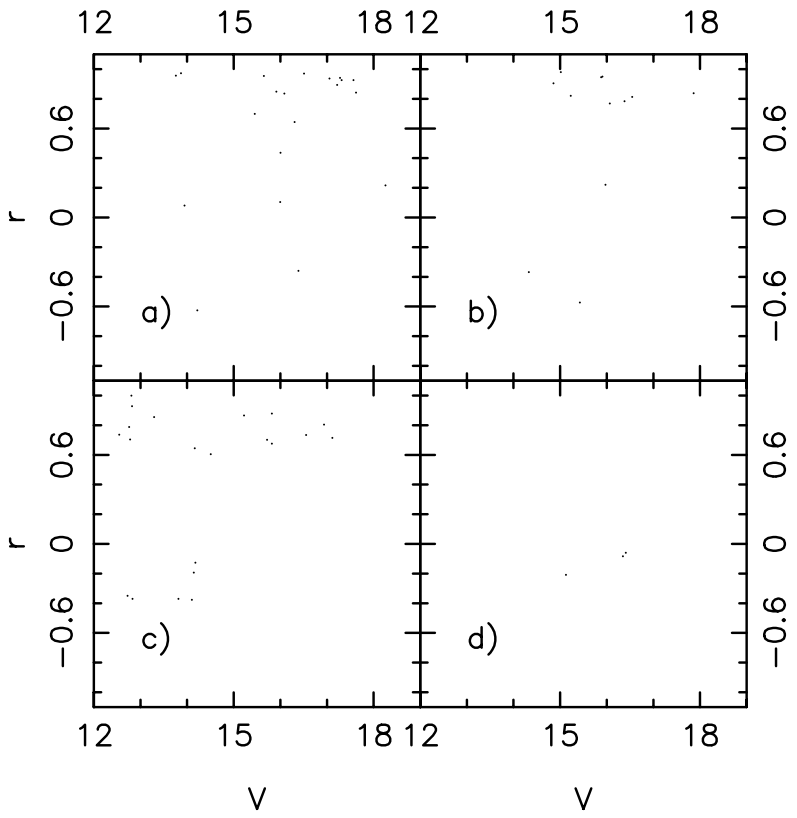

Figure 4.8: The correlation coefficient (r) as a function of magnitude for all candidate variables in all clusters studied. Panel a is for NGC 7789, b is for NGC 6819, c is for M67, and d is for NGC 188.

would also assume that the errors in V and those in B and R are uncorrelated and the errors are approximately the same size for each filter.) However, this is difficult to do at an arbitrary angle. Using the active stars in NGC 7789 as an example, I rotate the coordinate system of the V versus B panel of Figure 4.10 according to the fitted slope so that the high amplitude fluctuations due to the combination of signal and noise are along the x-axis and the noise is along the y-axis. An example of this is shown in Figure 4.11. The rotation was in the clockwise direction. The points that fell along the correlation are now located along the x-axis, and the noise is in the y-direction.

Now that I have effectively separated the the signal into one direction, I can estimate the strength of that signal by fitting Gaussians to the x- and y-distributions. Figure 4.12 shows histograms of the distributions for the panels of Figures 4.9 and 4.10 corresponding

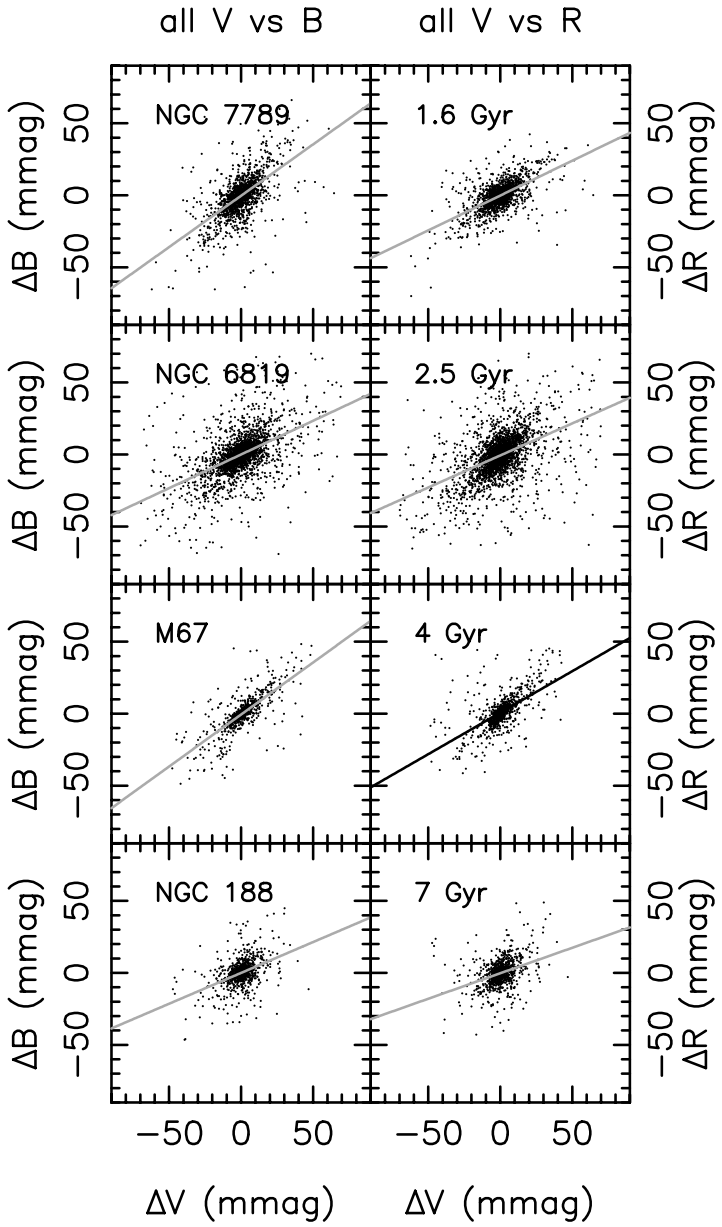

Figure 4.9: Mean V differential magnitudes versus mean B or R differential magnitudes for the main sequence stars in all the clusters. The left column of panels shows V vs B, and the right column of panels shows V vs R. The slopes of the lines can be found in Table 4.3. The main sequence stars in the three younger clusters show a distinct correlation between the colors, but the plot for NGC 188 shows only a hint of correlation.

Cluster	Population	Slope	χ^2_ν	# Points
NGC 7789	Main Seq. V vs B	0.71 ± 0.02	85	2470
	Main Seq. V vs R	0.48 ± 0.01	42	2495
	active V vs B	0.89 ± 0.04	87	233
	active V vs R	0.70 ± 0.03	50	230
NGC 6819	Main Seq. V vs B	0.47 ± 0.01	120	3555
	Main Seq. V vs R	0.45 ± 0.01	150	3590
	active V vs B	0.86 ± 0.06	130	127
	active V vs R	0.87 ± 0.05	78	129
M67	Main Seq. V vs B	0.72 ± 0.02	56	965
	Main Seq. V vs R	0.58 ± 0.03	83	916
	active V vs B	0.74 ± 0.03	72	235
	active V vs R	0.73 ± 0.04	120	235
NGC 188	Main Seq. V vs B	0.43 ± 0.03	62	1059
	Main Seq. V vs R	0.35 ± 0.03	67	1081

Table 4.3: Results of the line fits to the data in Figures 4.9 and 4.10 for all clusters studied. The lines were fit using the least squares method, which yields the slope and χ^2_ν. The last column is the number of data points plotted in each panel of the figure.

to NGC 7789, after they have been rotated according to the slopes of the best fit lines. The x- and y- directions are both plotted, the x as "signal + noise" and the y as "noise". I fit Gaussians to the binned signal+noise and noise distributions; the Gaussians are overplotted on the histograms. A visual inspection reveals that the full widths at half-maximum of the noise Gaussians are much smaller than those of the combination of signal and noise. The results of the fit are listed in Table 4.4.

The FWHMs for the active stars in the signal+noise direction are about five times larger larger than the FWHMs in the noise direction for the active stars. This difference is also present in the main sequence stars, although only about twice as large. For Gaussian signals and in the presence of Gaussian noise, the FWHM of the signal is related to those of the signal+noise and the noise by: $FWHM_s = \sqrt{FWHM^2_{s+n} - FWHM^2_n}$.

Consequently, I can calculate the FWHMs of the signal. The FWHMs for the signal in each signal+noise panel of Figures 4.12, 4.13, 4.14, and 4.15 are listed in Table 4.4. The FWHMs for the active stars are approximately four times larger than the FWHMs for the

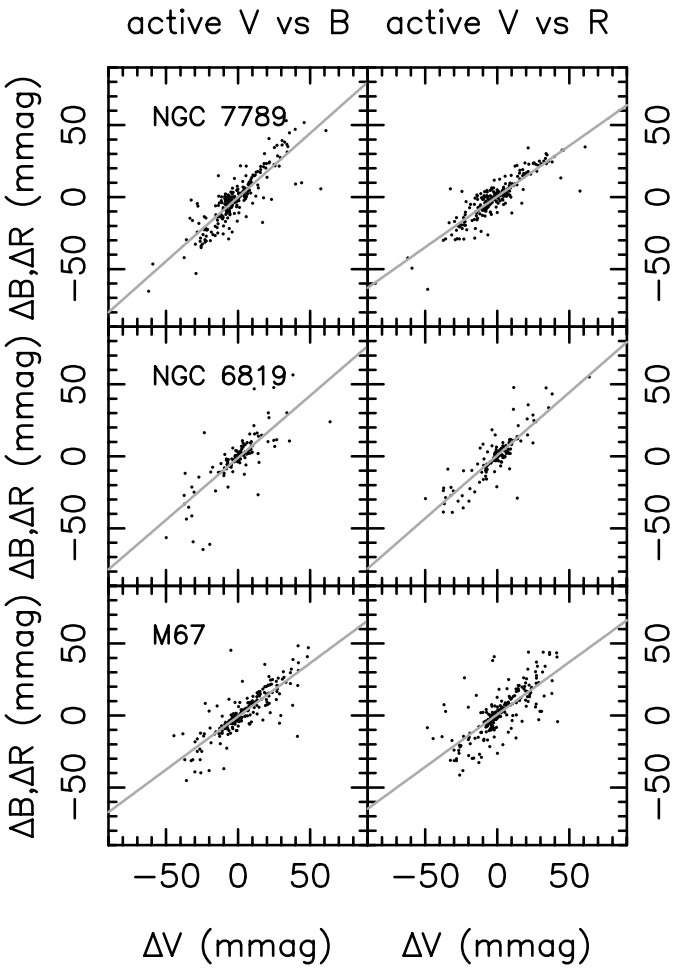

Figure 4.10: Mean V differential magnitudes versus mean B or R differential magnitudes for the active stars in all the clusters. The left column of panels shows V vs B, and the right column of panels show V vs R. NGC 188 has no active stars. The slopes of the lines can be found in Table 4.3.

main sequence stars in the same colors. The FWHMs for the V vs B distributions are somewhat larger than the FWHMs for the V vs R distributions at the same activity level. The FWHMs for the activity distribution can be used to evaluate the amount of activity in a cluster, even for stars that are not measurably active individually. The fact that the noise FWHMs for the active stars is larger than the noise FWHMs for the main sequence stars suggests that the error distribution does not have the same FWHM in each of the B, V, and R colors.

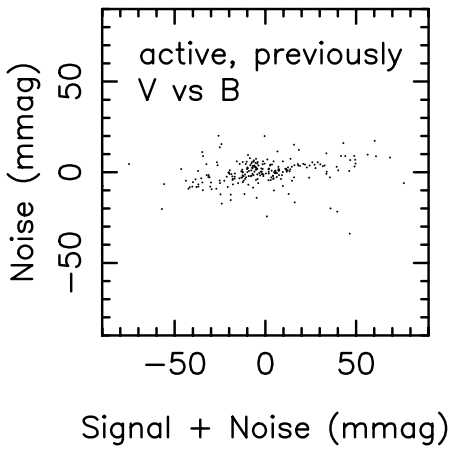

Figure 4.11: Rotated plot of V vs. B in the upper left panel of Figure 4.9. The points along the direction of correlation now lie on the x-axis and are attributed to the combination of the signal and noise. The points perpendicular to the direction of correlation now fall on the y-axis and are attributed to the noise in the observations.

4.2.2 Solar Analogs

The nightly mean differential magnitudes are plotted for selected solar analog stars in each cluster. However, since the Phase II data were taken over a limited period of time, the lightcurves do not display significant trends.

NGC 7789

As in Phase I, solar-type stars in NGC 7789 will fall in the range $17 < V < 17.5$ and $0.8 <$ B-V < 1.1. The combined BVR data are shown for a few solar analogs in Figure 4.16. The day number starts from UT 2001 Dec 17 as Day 0 and runs through December 2002. Since only a few observations were made in December 2001, the plots only display observations for September through December 2002. Table 4.5 lists information about each star.

NGC 6819

Solar-type stars in NGC 6819 fall in the range $16.75 < V < 17.25$ and $0.65 <$ B-V $<$ 0.95. The combined BVR data are shown for a few solar analogs in Figure 4.17. The day

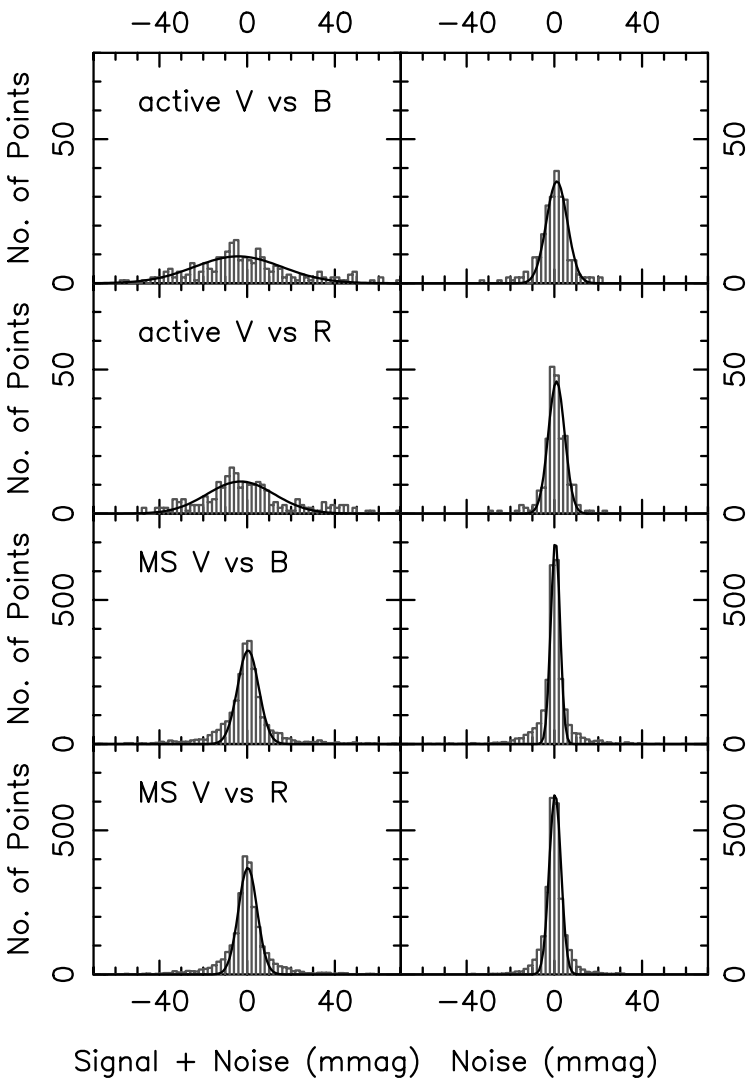

Figure 4.12: Histograms of the distributions in the panels of Figures 4.9 and 4.10 for NGC 7789 after the points have been rotated such that the positive correlation lies along the x-axis. Gaussian fits have been superimposed. Table 4.4 lists the fit results.

number starts from UT 2002 Aug 12 as Day 0 and runs through November 2002. Table 4.6 lists information about each star.

M67

In M67, solar-type stars have $14 < V < 15.25$ and $0.55 < B\text{-}V < 0.85$. A few solar analogs are shown in Figure 4.18. The day number starts from UT 2001 Dec 16 and runs through

Cluster	Population	Colors	FWHM, signal+noise (mmag)	FWHM, noise (mmag)	FWHM, signal (mmag)
NGC 7789	active	V vs B	66.73	15.98	64.79
	active	V vs R	51.08	12.46	49.54
	main seq.	V vs B	16.11	6.93	14.54
	main seq.	V vs R	14.25	8.87	11.15
NGC 6819	active	V vs B	33.15	9.75	31.68
	active	V vs R	38.05	11.04	36.41
	main seq.	V vs B	18.09	9.82	15.19
	main seq.	V vs R	19.41	14.73	12.64
M67	active	V vs B	58.23	10.20	57.33
	active	V vs R	65.80	13.99	64.30
	main seq.	V vs B	18.02	5.84	17.05
	main seq.	V vs R	20.03	10.94	16.78
NGC 188	main seq.	V vs B	15.46	10.47	11.38
	main seq.	V vs R	15.36	13.87	6.60

Table 4.4: Results of the fits of the Gaussians to the histograms in Figures 4.12, 4.13, 4.14, and 4.15. The FWHMs are much larger for the populations with signal+noise, as would be expected. The FWHM for the signal was determined as described in § 4.2.1.

Star	V	B-V	# of Nights	α_v	r	99% sig?	A_v	A_b	A_r
2437	17.428	0.971	20	1.28	0.02	N	5.4	5.3	6.1
2627	17.265	0.929	20	2.06	0.70	Y	9.0	12.0	8.9
2965*	17.369	0.901	20	3.19	0.93	Y	6.3	31.2	25.8

Table 4.5: Solar analogs in NGC 7789. Solar analogs are plotted in Figure 4.16. α_v is the significance index. r is the correlation coefficient, and the "99% sig?" column indicates whether or not the correlation is significant at the 99% level. All stars were observed the same number of nights through each filter. The last three columns are the activity indices of each star through each filter. An asterisk denotes an active star.

2003 Mar 15. Table 4.7 lists information about each star.

NGC188

The solar-type stars in NGC 188 fall in the range $16.0 < V < 16.5$ and $0.6 <$ B-V < 0.9. Three solar analogs are shown in Figure 4.19. The day number runs from UT 2001 Dec 17 as Day 0 through UT 2003 Jan 14. Table 4.8 lists information about each star.

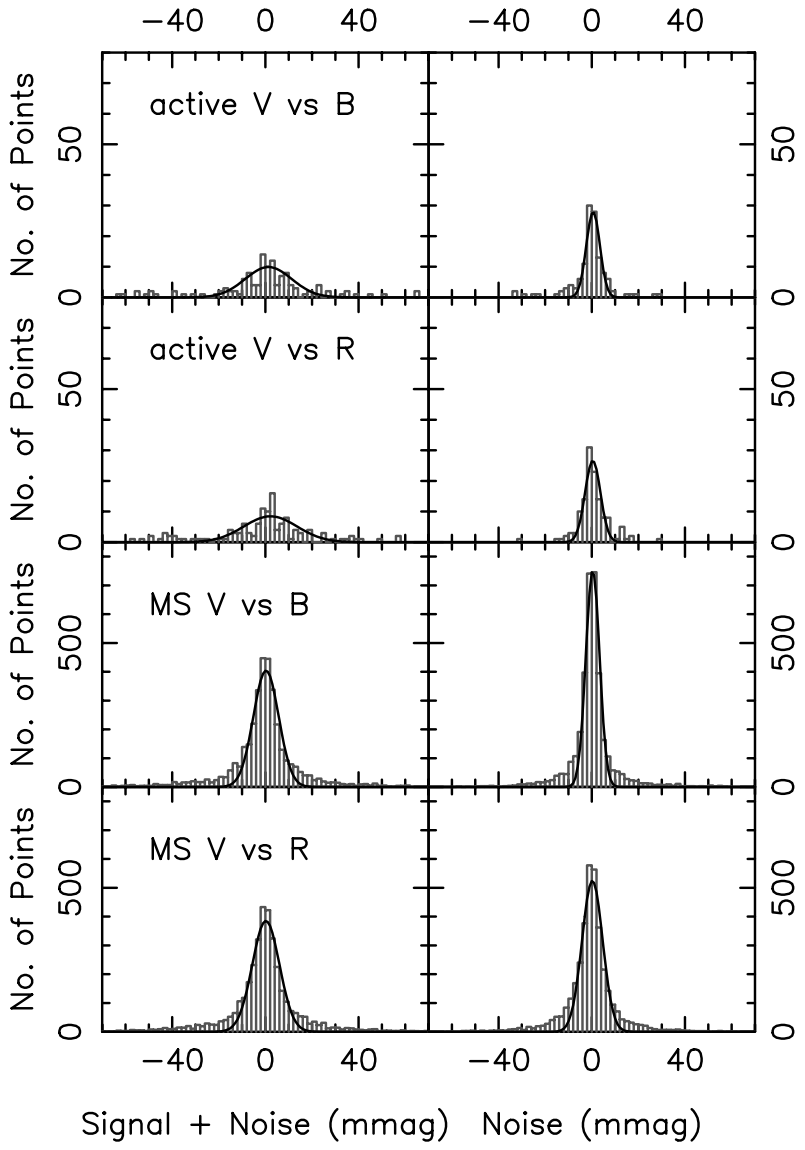

Figure 4.13: Histograms of the distributions for NGC 6819 in the panels of Figures 4.9 and 4.10 after the points have been rotated such that the positive correlation lies along the x-axis. Gaussian fits have been superimposed. Table 4.4 lists the fit results.

4.3 Activity on the Yearly Timescale

4.3.1 The Activity Determination

The previous analysis of the nightly mean magnitudes of the stars in each cluster revealed the stellar activity present on the rotational timescale. In order to search for solar-cycle

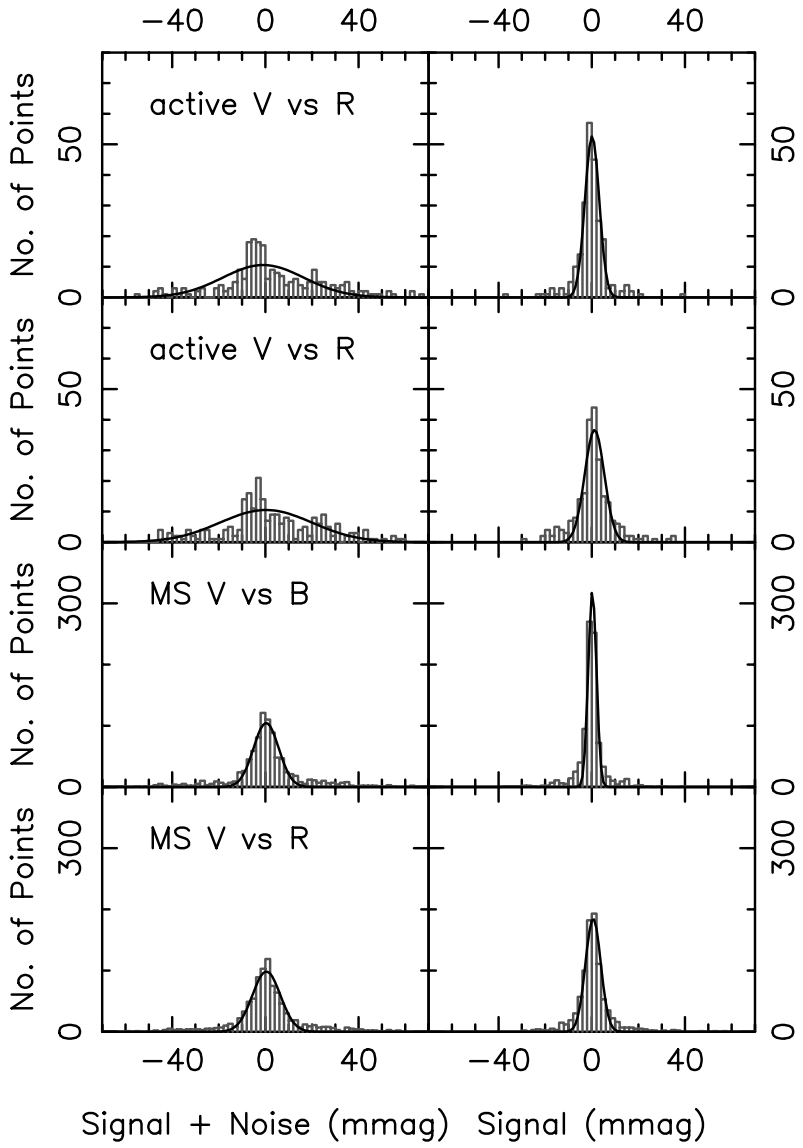

Figure 4.14: Histograms of the distributions for M67 in the panels of Figures 4.9 and 4.10 after the points have been rotated such that the positive correlation lies along the x-axis. Gaussian fits have been superimposed. Table 4.4 lists the fit results.

variability, I must analyze the annual mean differential magnitudes. Combining Phase I and Phase II data, the data set consists of eight years of observations in B, V, R, and I for some stars. I have included R data from Phase I as listed in Table 4.9. Examination of the photometry check file for NGC 6819 revealed that nights UT 2001 Jul 18 and UT 2001 Oct 13 had median magnitudes in R considerably higher than the other frames and

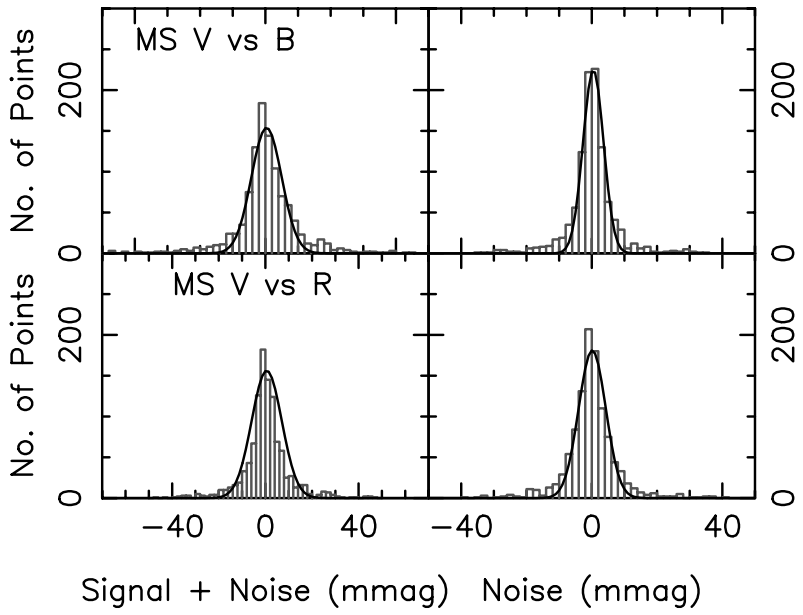

Figure 4.15: Histograms of the distributions for NGC 188 in the panels of Figure 4.9 after the points have been rotated such that the positive correlation lies along the x-axis. Gaussian fits have been superimposed. Table 4.4 lists the fit results.

Star	V	B-V	# of Nights	α_v	r	99% sig?	A_v	A_b	A_r
3465	16.768	0.760	16	1.30	0.37	N	5.9	5.4	4.6
3128	16.866	0.790	16	1.37	-0.15	N	6.2	4.7	5.6
2959	16.868	0.865	16	1.91	0.73	Y	10.6	9.2	10.0

Table 4.6: Solar analogs in NGC 6819. Solar analogs are plotted in Figure 4.17. The number of nights each star was observed is listed. α_v is the significance index. r is the correlation coefficient, and the column "99% sig?" indicates whether or not the correlation is significant at the 99% level. The last three columns are the activity indices for the star for each filter. An asterisk denotes an active star.

should be removed. Similarly, UT 2000 Jun 27 and UT 2000 Dec 12 were removed from the I data. No other data listed in the table were discarded for any of the clusters.

I use a procedure analogous to that performed on the nightly mean magnitude data to identify active stars. I calculate the activity index and significance index as before, requiring stars to have at least five seasons of V observations to be included. No ensemble error was included in the calculation.

Since data in four colors are available, the linear correlation coefficient is applied to B,

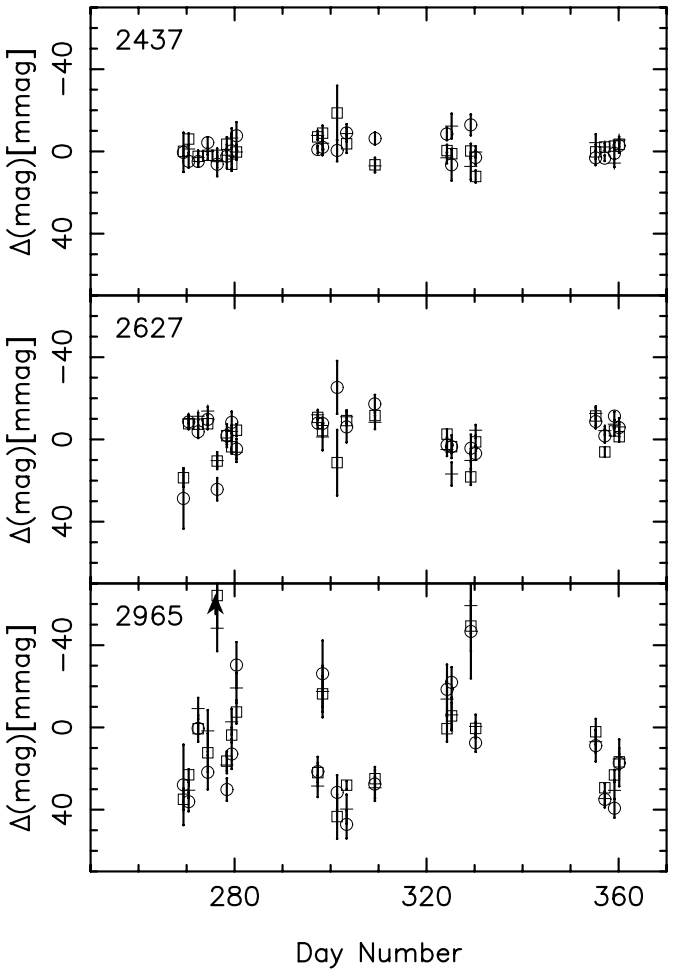

Figure 4.16: Nightly mean BVR data for selected stars in NGC 7789. The crosses are V data, the circles are B data, and the boxes are R data. Y-axis units are in millimagnitudes. Error bars are included on all points.

V, R, and I. The coefficient is only calculated for stars with at least five pairs of BV, VR, and/or VI annual mean differential magnitude pairs. Figure 4.20 shows the correlation coefficient as a function of V magnitude for the main sequence each of the clusters. The majority of stars in NGC 7789 and NGC 6819 are positively correlated. The stars in M67 have random correlations, although the few number of stars makes it difficult to be certain. The stars in NGC 188 also have random correlations. Figure 4.21 shows the correlation coefficients for the candidate variable stars in each cluster. This plot is similar to Figure 4.20, just with fewer stars plotted. Most of the candidate variables in M67 are

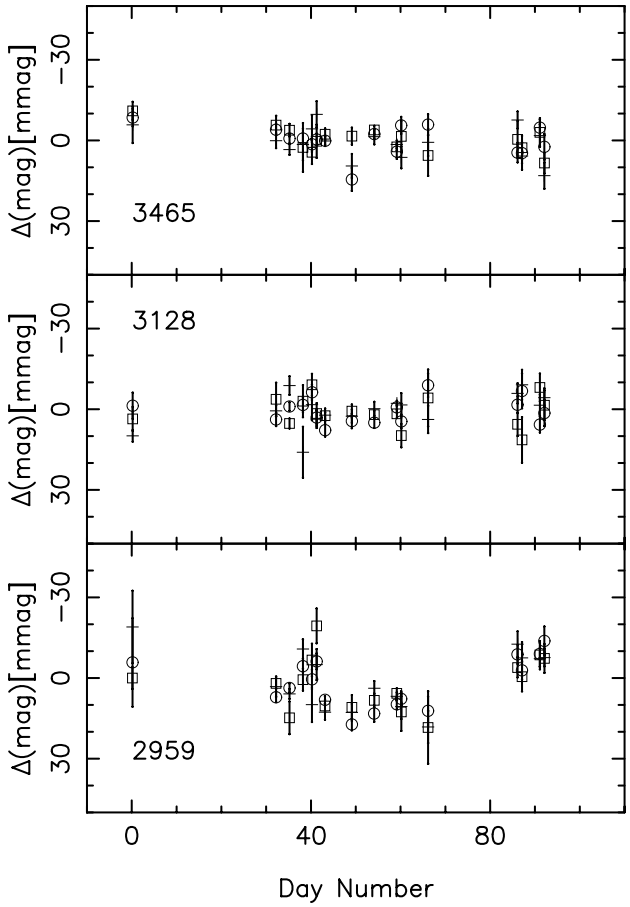

Figure 4.17: Nightly mean BVR data for selected solar analogs in NGC 6819. The crosses are V data, the circles are B data, and the boxes are R data. Information about the stars is listed in Table 4.6.

positively correlated at higher magnitudes; the candidate variables in NGC 188 show only random scatter.

A summary of the activity on the annual timescale in give in Table 4.10. NGC 7789 and NGC 6819 have a relatively large percentage of active stars on the annual timescale, while M67 and NGC 188 have a very small fraction. Figure 4.22 shows the main sequence stars in each cluster (observed at least five seasons in V) and the active stars in each cluster. The two active stars in M67 fall on the main sequence turn-off. One of the active stars in NGC 188 also falls on the main sequence turn-off.

Figure 4.23 plots the annual mean V magnitudes versus the annual mean B, R, or I magnitudes for the active stars in each cluster. (Since M67 only had two active stars, all

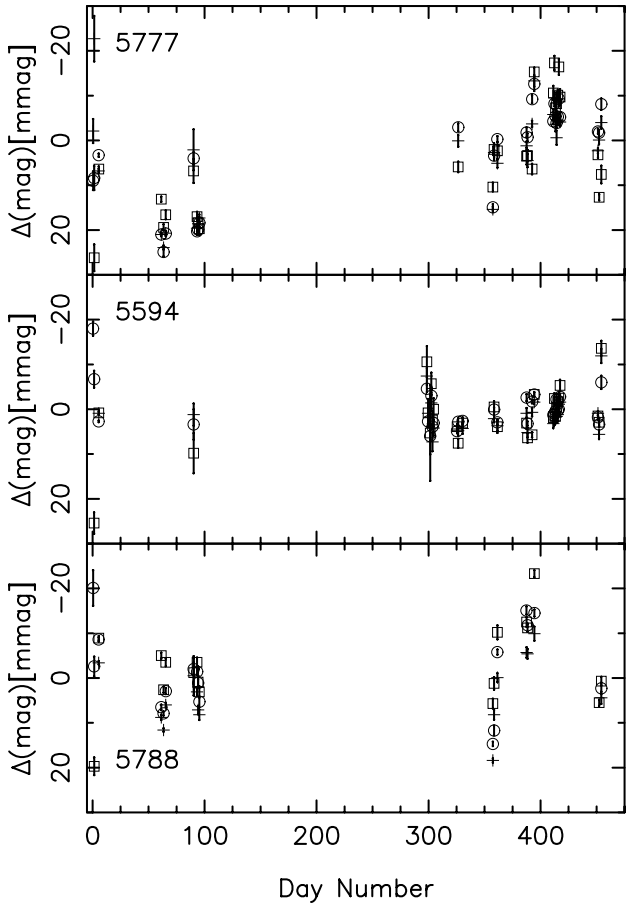

Figure 4.18: Nightly mean BVR data for selected stars in M67. The crosses are V data, the circles are B data, and the boxes are R data. Y-axis units are in millimagnitudes. Error bars are included on all points.

points are plotted on the same panel, regardless of the color.) The scatter is somewhat reduced in these plots and the positive correlation is more obvious, especially in NGC 7789 and NGC 6819. Lines were fitted to each panel; the fit results are listed in Table 4.11.

4.3.2 Interesting Stars

To get a feel for the behavior of the stars over the seven-year period, I selected the four stars with the lowest significance indices and the four stars with the highest significance indices in each cluster; I only chose stars with at least seven seasons for NGC 7789 and NGC 6819 and at least eight seasons for M67 and NGC 188. The stars are plotted in Figures 4.24, 4.25, 4.26, and 4.27. The V magnitudes and colors of the stars, as well as

Star	V	B-V	# of Nights	α_v	r	99% sig?	A_v	A_b	A_r
5777*	14.516	0.737	28	4.41	0.61	Y	11.7	11.4	14.6
5594	14.160	0.708	29	5.40	-0.19	N	14.5	4.7	10.2
5788	14.183	0.711	17	6.18	-0.13	N	18.0	9.7	16.2

Table 4.7: Solar analogs in M67. Solar analogs are plotted in Figure 4.18. The number of nights each star was observed is listed. α_v is the significance index. r is the correlation coefficient, and the column "99% sig?" indicates whether or not the correlation is significant at the 99% level. The last three columns are the activity indices for the star for each filter. An asterisk denotes an active star.

Star	V	B-V	# of Nights	α_v	r	99% sig?	A_v	A_b	A_r
645	16.335	0.760	20	0.85	-0.02	N	3.9	7.9	5.5
709	16.059	0.821	20	1.54	0.77	Y	4.9	5.7	4.9
648	16.436	0.766	20	3.00	-0.06	N	12.8	9.5	8.5

Table 4.8: Solar analogs in NGC 188. Solar analogs are plotted in Figure 4.19. α_v is the significance index. r is the correlation coefficient, and the column "99% sig?" indicates whether or not the correlation is significant at the 99% level. The last three columns are the activity indices for the data taken through each filter.

Telescope	Dates (UT)	CCD	Objects
Perkins	1998 Oct 14	SITe	1, 2, 3, 4
Perkins	1998 Oct 19	SITe	1, 2, 3, 4
Perkins	1999 Oct 14	SITe	1, 2, 3, 4
Perkins	2000 Oct 26	Loral1	2, 3, 4
Perkins	2001 Jul 18	Loral2	2
Perkins	2001 Oct 13	Loral2	1, 2, 3, 4

Table 4.9: Phase I R observations that were added to the Phase I BVI and Phase II BVR data when the data sets were combined for the yearly analysis. "Perkins" refers to the 1.8-m Perkins Telescope at Lowell Observatory. The CCD designations "SITe", "Loral1", and "Loral2" are explained in the text. The clusters are assigned numbers in order of age: 1 – NGC 7789, 2 – NGC 6819, 3 – M67, 4 – NGC 188.

their significance indices and correlation coefficients, are listed in Tables 4.12, 4.13, 4.14, and 4.15.

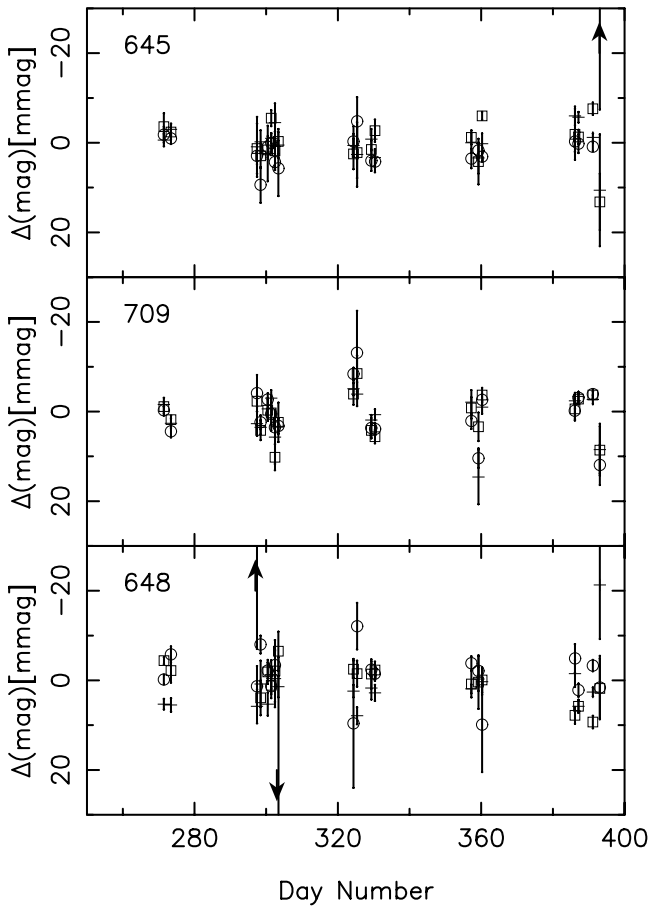

Figure 4.19: Nightly mean BVR data for selected stars in NGC 188. The crosses are V data, the circles are B data, and the boxes are R data. Y-axis units are in millimagnitudes. Error bars are included on all points.

4.3.3 Solar Analogs

Since I am searching for variability similar to the solar cycle, I look at the annual mean BVRI differential magnitudes for solar analogs in each cluster. Again, I only look at stars with at least seven seasons of V observations for NGC 7789 and NGC 6819 and at least eight seasons of V observations for M67 and NGC 188. The solar analogs were chosen the same way as for the nightly mean magnitude data (see Table 3.15). Information about the stars is in Tables 4.16, 4.17, 4.18, and 4.19, for NGC 7789, NGC 6819, M67, and NGC 188, respectively. Since in some clusters have a number of stars considered to be solar analogs and with sufficient V data, some of the clusters have multiple plots of the BVRI annual

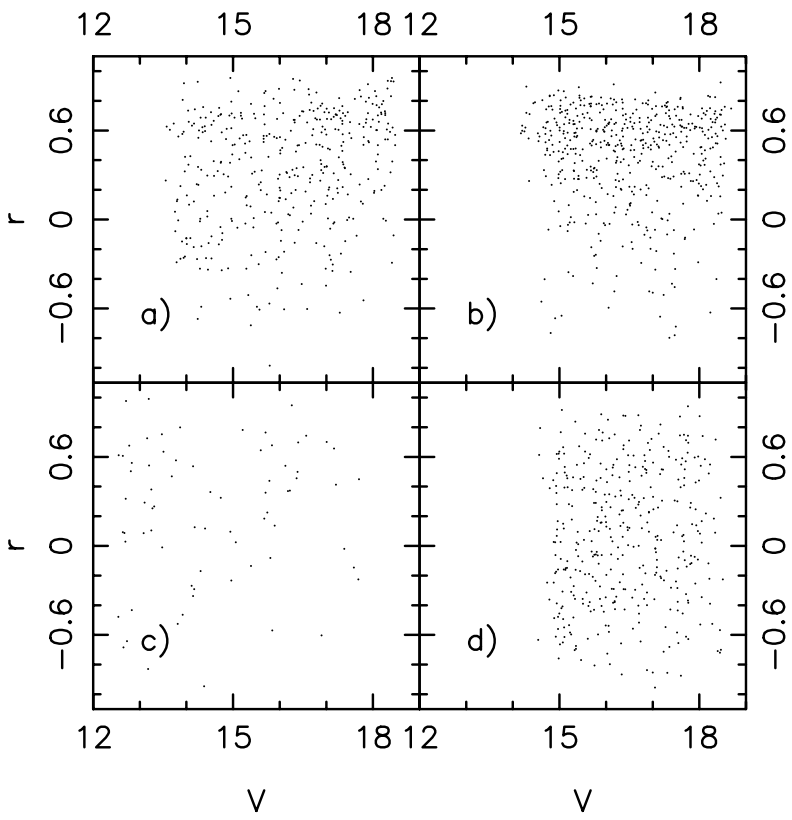

Figure 4.20: The correlation coefficient (r) as a function of magnitude for the annual mean differential magnitudes of the main sequence stars in all clusters studied. Panel a is NGC 7789, b is NGC 6819, c is M67, and d is NGC 188.

means data. The solar analogs for NGC 7789 are shown in Figures 4.28 and 4.29. The solar analogs for NGC 6819 are shown in Figures 4.30, 4.31 and 4.32. For M67, the solar analogs are shown in Figures 4.33 and 4.34. Finally, the solar analogs for NGC 188 are shown in Figure 4.35. All of the plots have different y-scales.

With up to eight seasons of data for some of the clusters, the lightcurves now have a long enough time base to show interesting behavior. In NGC 7789, star 2486 is declining in brightness (Figure 4.28), and star 3245 (Figure 4.29) may be showing a nearly-complete cycle. In NGC 6819, stars 3128 (Figure 4.30) and 3605 (Figure 4.31) show irregular variations very well-correlated between the colors. Star 4254 (Figure 4.32) shows a downward trend over the seven seasons. In M67, star 5768 shows no variability over about 7 mmag

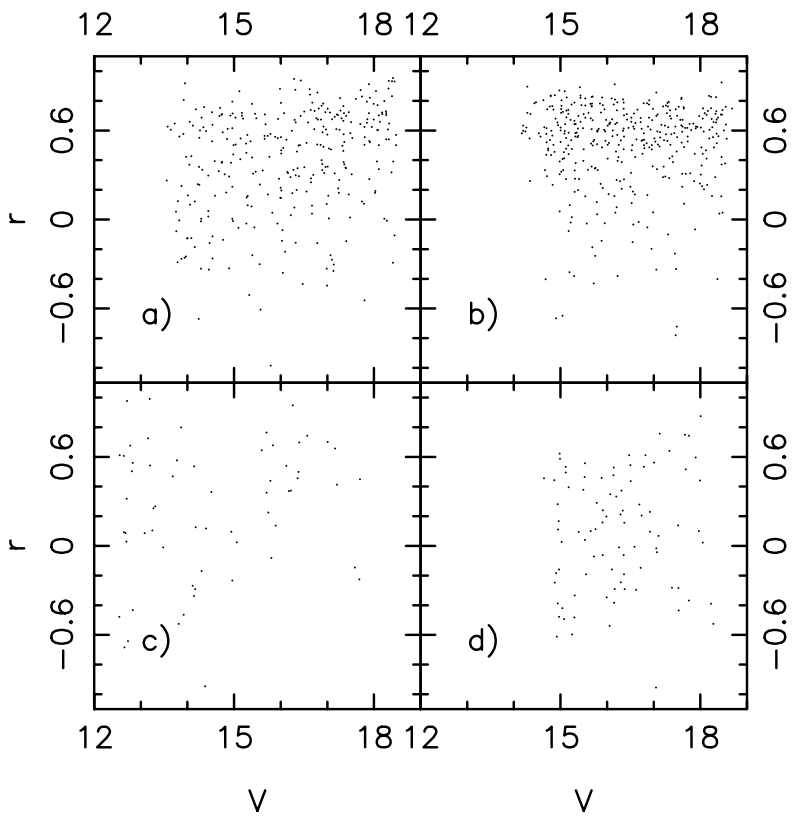

Figure 4.21: The correlation coefficient (r) as a function of magnitude for the annual mean differential magnitudes of the candidate variables in all clusters studied. Panel a is NGC 7789, b is NGC 6819, c is M67, and d is NGC 188.

in any color during the whole eight-year period. In NGC 188, star 549 shows irregular fluctuations well-correlated between colors at a level of approximately 10 mmag.

Cluster	# MS	# Cand. Var.	# MS	# 99% sig.	# Active
NGC 7789	393	308 (78%)	391	55 (14%)	51 ± 7 (12%)
NGC 6819	513	384 (75%)	511	105 (21%)	99 ± 10 (19%)
M67	82	69 (84%)	73	4 (5%)	2 ± 1 (3%)
NGC 188	192	88 (46%)	380	6 (2%)	5 ± 2 (3%)

Table 4.10: Summary of Annual Activity for Phase II. The second column lists the number of main sequence stars with at least five seasons of observations in V that were included in the activity index calculation. The third column is the number of candidate variable stars found. The fourth column is the number of main sequence stars with at least five pairs of B and V and/or V and R observations in the same season; these stars were included in the correlation coefficient calculation. The fifth column is the number of stars whose correlation coefficients were 99% significant. The last column listing the fraction of active stars uses the lower of the two main sequence star numbers. The uncertainty in the number of active stars is the square root of the number.

Cluster	Population	Slope	χ^2_ν	# Points
NGC 7789	Active V vs B	1.03 ± 0.08	170	253
	Active V vs R	0.62 ± 0.06	86	191
	Active V vs I	0.86 ± 0.06	70	193
NGC 6819	Active V vs B	0.73 ± 0.04	200	513
	Active V vs R	0.25 ± 0.05	160	320
	Active V vs I	0.71 ± 0.06	200	304
M67	Active all	1.10 ± 0.11	1.3	10
NGC 188	Active V vs B	0.61 ± 0.17	120	28
	Active V vs R	0.73 ± 0.17	150	27
	Active V vs I	1.25 ± 0.25	98	17

Table 4.11: Results of the line fits to the data in Figure 4.23 for all clusters studied. The lines were fit according to the least squares method. The last column is the number of data points plotted in each panel of the figure.

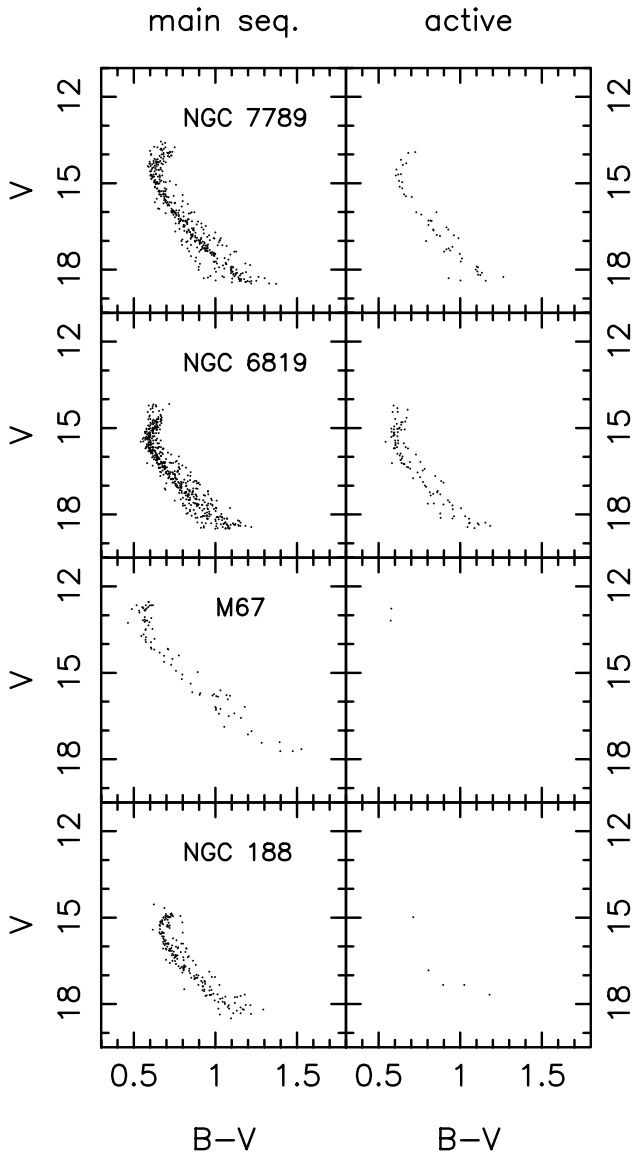

Figure 4.22: Color-magnitude diagrams for each cluster based on the annual data. The left column of panels shows the main sequence stars observed on at least five seasons through the V filter for each cluster. The right column of panels shows the stars found to be active in each cluster.

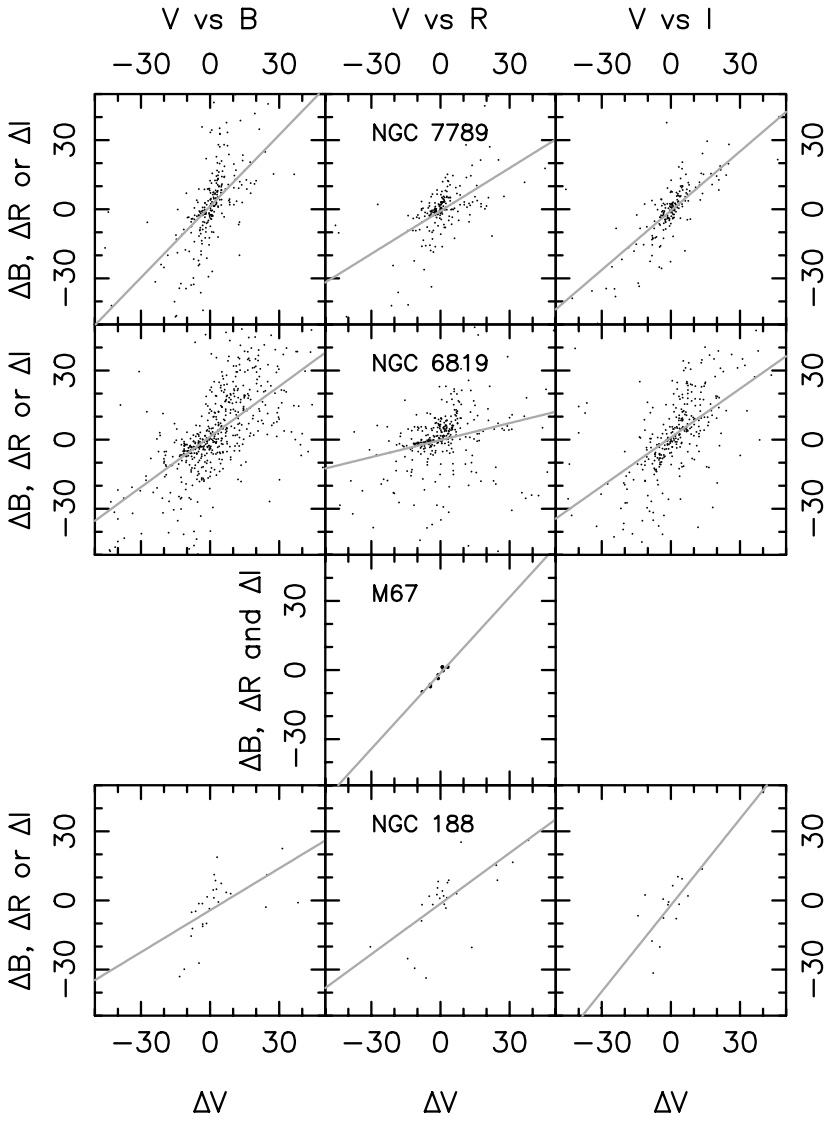

Figure 4.23: Annual mean V differential magnitudes versus mean B, R or I differential magnitudes for the main sequence stars in each cluster. The left column of panels shows the annual mean V magnitudes versus the annual mean B magnitudes; the middle column of panels shows V versus R, and the right column of panels shows V versus I. M67 only has two active stars, so all color are plotted in the middle panel. The rows of panels corresponds to the four clusters, from the top to bottom row: NGC 7789, NGC 6819, M67, and NGC 188. Units are in mmags. Results of the line fits can be found in Table 4.11.

Star	V	B-V	α_v	r	99% sig?	# R	A_v
2188	16.698	0.843	1.11	0.57	N	4	3.6
2212	16.327	0.893	1.13	0.67	N	3	3.0
2458	13.963	0.713	1.16	0.32	N	4	1.4
2259	16.506	0.809	1.37	-0.01	N	4	1.6
2211	17.510	0.991	16.77	0.55	N	4	32.4
3336*	14.361	0.649	17.86	0.76	Y	4	6.5
3199*	18.183	1.123	18.72	0.87	Y	3	84.8
2525*	16.605	0.927	34.96	0.84	Y	4	23.0

Table 4.12: Interesting stars in NGC 7789 on the yearly timescale. The stars are plotted in Figure 4.24. α_v is the significance index, and r is the correlation coefficient. The "99% sig?" column indicates whether the correlation is significant at the 99% level. All stars have seven season of observations in V. All stars have six seasons of observations in B, except 3199, which has five. All stars have four seasons of observations in I. The table indicates the number of seasons of observations in R. The last column lists the activity indices for the V annual means. An asterisk denotes an active star.

Star	V	B-V	α_v	r	99% sig?	# B	# R	A_v
4055	16.065	0.654	0.71	0.50	N	7	4	3.6
3108	16.920	0.885	1.19	0.66	N	6	3	9.7
3860	17.095	0.864	1.29	0.13	N	6	4	5.5
2710	15.624	0.587	1.39	0.03	N	6	4	2.7
3304*	15.016	0.577	13.18	0.87	Y	7	3	44.7
4236*	17.231	0.814	13.22	0.79	Y	7	2	98.8
3764*	15.046	0.593	13.72	0.80	Y	7	4	23.0
3212*	18.432	1.045	14.87	0.75	Y	7	4	279.8

Table 4.13: Interesting stars in NGC 6819 on the yearly timescale. The stars are plotted in Figure 4.25. α_v is the significance index, and r is the correlation coefficient. The "99% sig?" column indicates whether the correlation is significant at the 99% level. All stars have seven seasons of observations in V and four seasons in I. The table indicates the number of seasons of observations in B and R. The last column lists the activity indices for the V annual means. An asterisk denotes an active star.

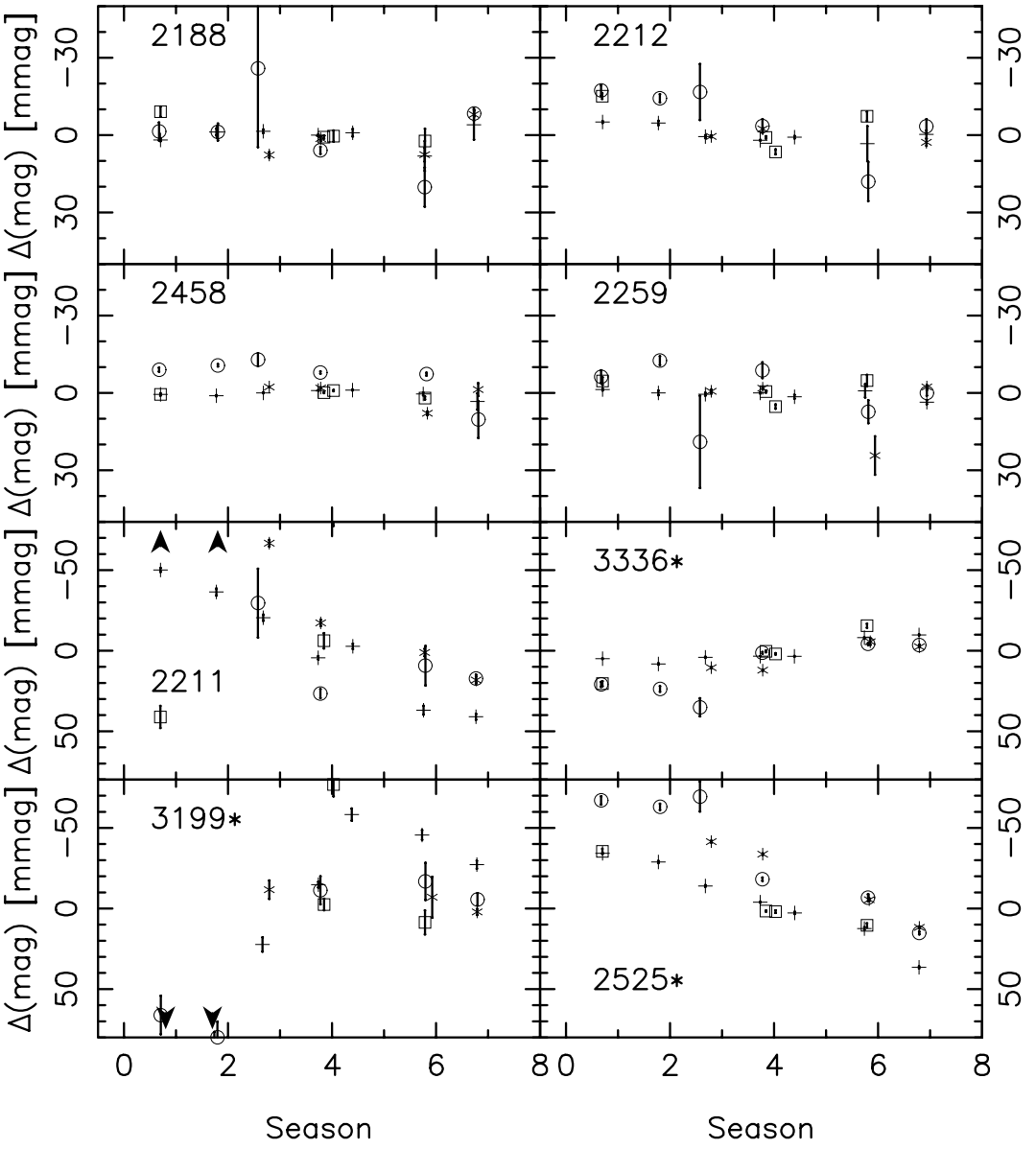

Figure 4.24: Interesting stars in NGC 7789 on the yearly timescale. Stars are ordered by increasing significance index. Season 0 is 1996. Star properties are listed in Table 4.12. An asterisk denotes and active star. Units on y-axis are millimagnitudes. Error bars are included on all points. An arrow indicates where a point falls off the plot. Crosses are V, circles are B, boxes are I, and asterisks are R.

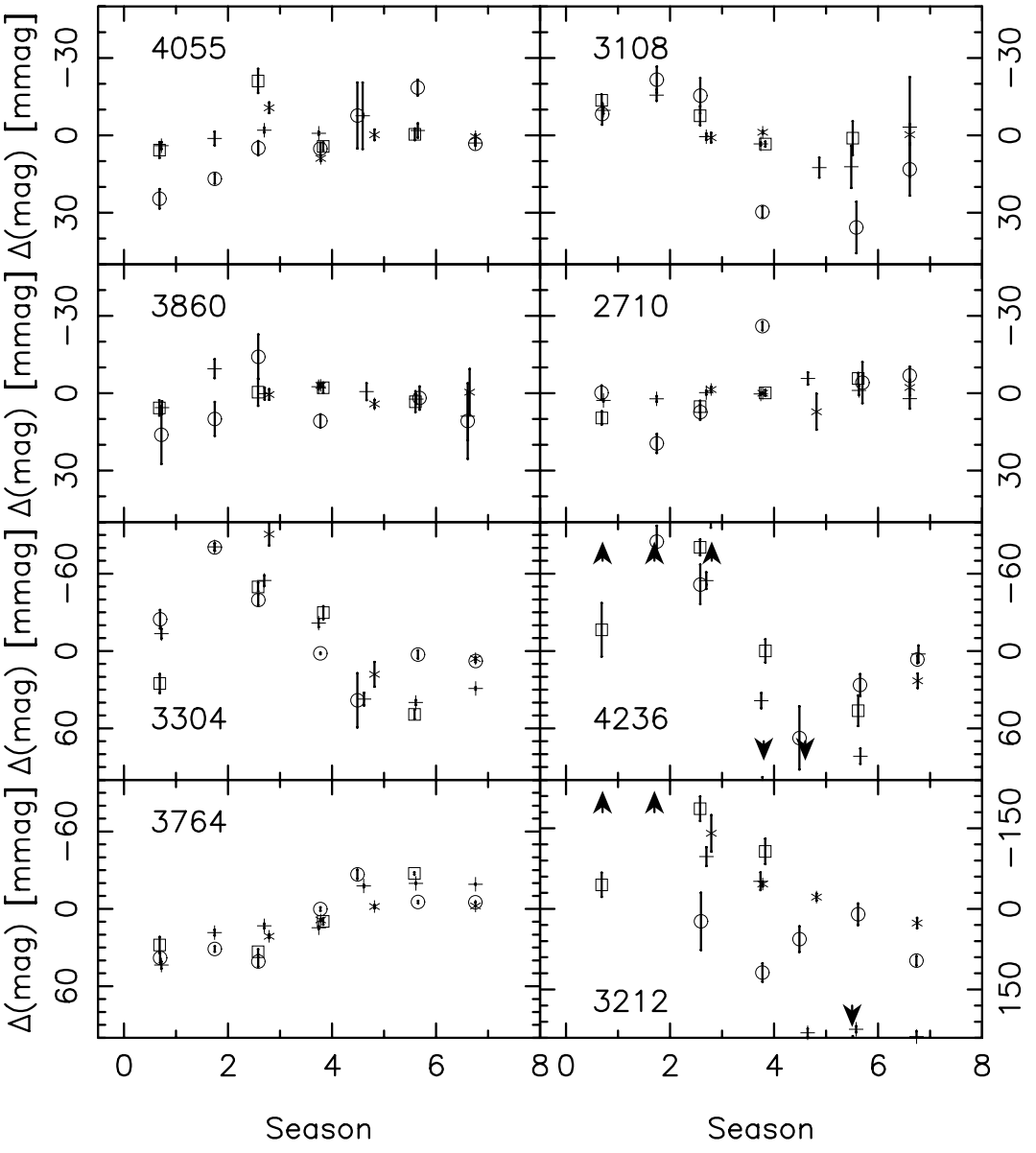

Figure 4.25: Interesting stars in NGC 6819 on the yearly timescale. Season 0 is 1996. Star properties are listed in Table 4.13. An asterisk denotes and active star. Units on y-axis are millimagnitudes. Error bars are included on all points. An arrow indicates where a point falls off the plot. Crosses are V, circles are B, boxes are I, and asterisks are R.

Star	V	B-V	α_v	r	99% sig?	# R	A_v
5695	13.095	0.608	1.68	0.29	N	3	4.1
5763	13.477	0.614	1.75	0.75	N	6	2.0
5562	12.805	0.572	3.03	0.56	N	6	5.2
5620	15.779	1.068	4.13	-0.08	N	6	4.5
5653	13.666	0.560	13.80	0.47	N	6	5.8
5790	12.533	0.589	15.22	0.61	N	6	4.6
5691	15.828	1.016	15.39	0.68	N	5	16.6
5675	12.755	0.559	29.64	0.68	N	6	10.1

Table 4.14: Interesting stars in M67 on the yearly timescale. The stars are plotted in Figure 4.26. α_v is the significance index, and r is the correlation coefficient. The "99% sig?" column indicates whether the correlation is significant at the 99% level. All stars have eight season of observations in V. All stars have four seasons of observations in B, except 5695, which has two. All stars have two seasons of observations in I, except 5695, which has one. The table indicates the number of seasons of observations in R. The last column lists the activity indices for the V annual means. An asterisk denotes an active star.

Star	V	B-V	α_v	r	99% sig?	A_v
829	17.680	0.967	1.16	0.41	N	7.9
851	16.103	0.700	1.24	0.26	N	11.2
648	16.436	0.766	1.53	-0.29	N	2.6
812	15.300	0.701	1.68	-0.27	N	5.3
610*	17.668	1.180	6.40	0.75	Y	18.5
856	15.765	0.686	6.58	0.11	N	12.4
645	16.335	0.760	9.50	0.24	N	11.7
767*	17.337	1.025	31.08	0.76	Y	87.9

Table 4.15: Interesting stars in NGC 188 on the yearly timescale. The stars are plotted in Figure 4.27. α_v is the significance index, and r is the correlation coefficient. The "99% sig?" column indicates whether the correlation is significant at the 99% level. All stars have eight season of observations in V. All stars have seven seasons of observations in B, except 610, which has six. All stars have six seasons of observations in R. All stars have four seasons of observations in I, except 856, which has three. The last column lists the activity indices for the V annual means. An asterisk denotes an active star.

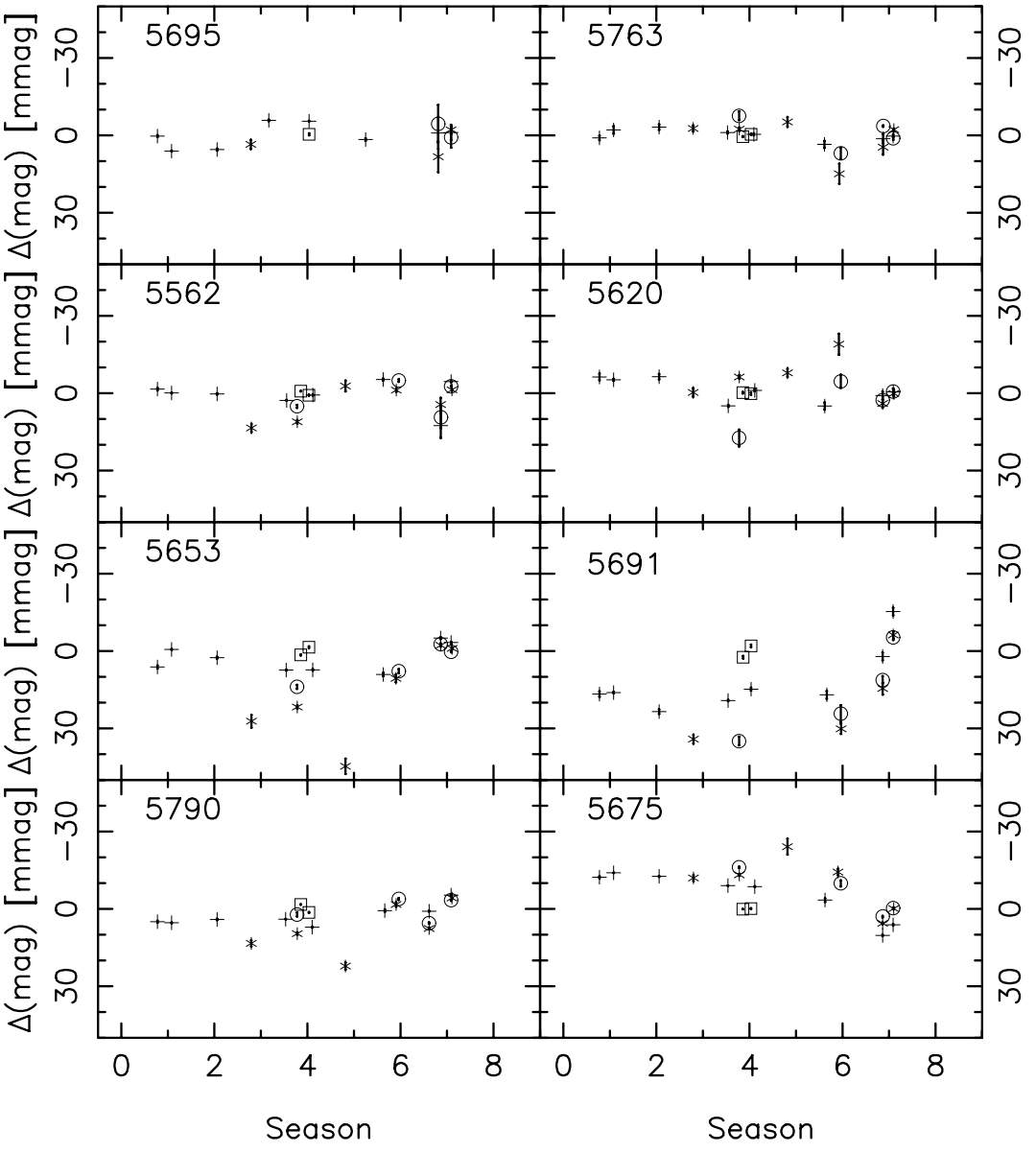

Figure 4.26: Interesting stars in M67 on the yearly timescale. Season 0 is 1996. Star properties are listed in Table 4.14. An asterisk denotes and active star. Units on y-axis are millimagnitudes. Error bars are included on all points. An arrow indicates where a point falls off the plot. Crosses are V, circles are B, boxes are I, and asterisks are R.

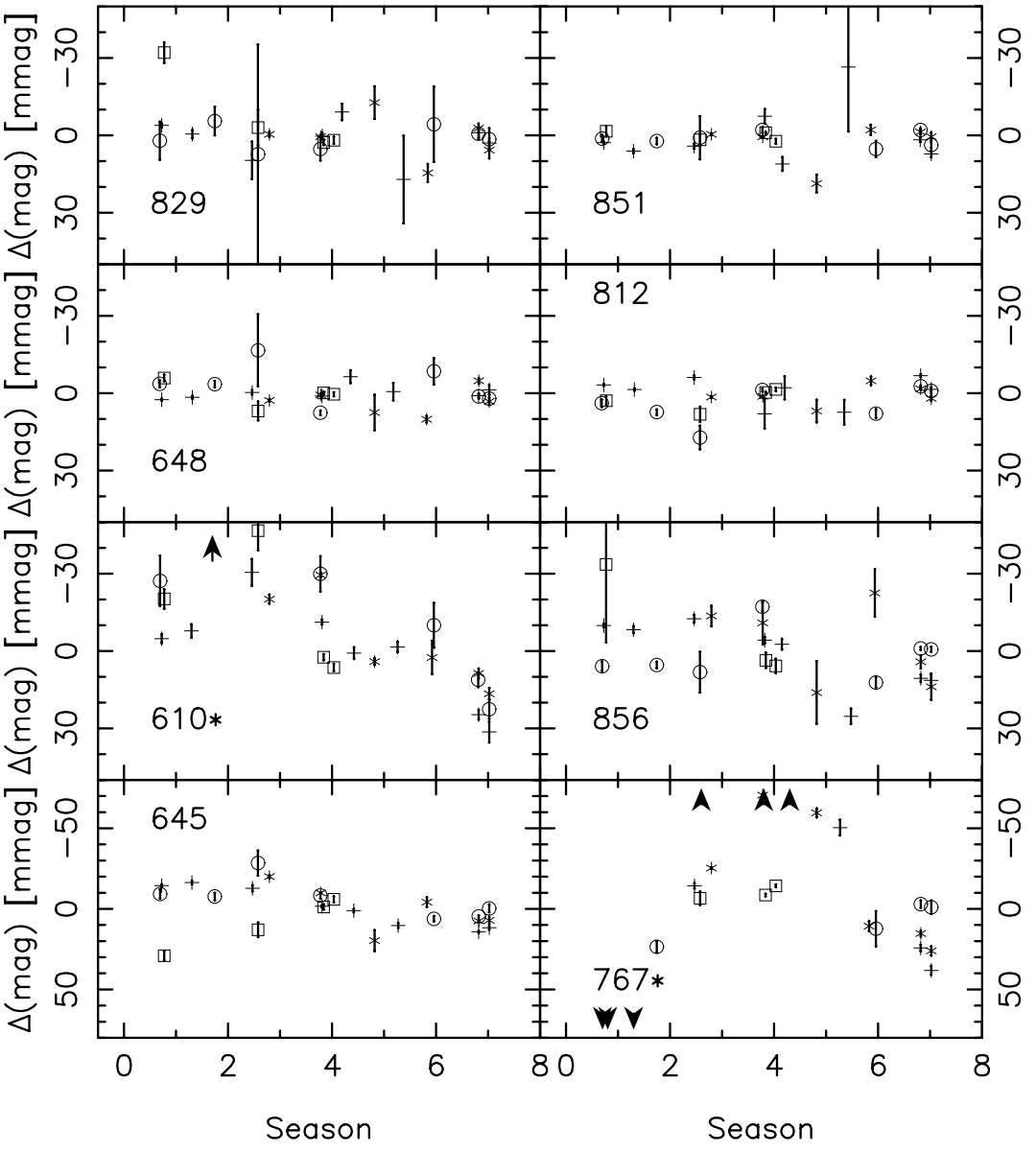

Figure 4.27: Interesting stars in NGC 188 on the yearly timescale. Season 0 is 1996. Star properties are listed in Table 4.15. An asterisk denotes and active star. Units on y-axis are millimagnitudes. Error bars are included on all points. An arrow indicates where a point falls off the plot. Crosses are V, circles are B, boxes are I, and asterisks are R.

Star	V	B-V	α_v	r	99% sig?	A_v
2959	17.346	0.942	3.37	0.46	N	5.5
3467	17.132	0.954	4.20	-0.35	N	4.1
2486	17.350	0.938	4.38	0.39	N	6.6
2235*	17.206	0.952	4.88	0.71	Y	7.8
2930	17.398	0.977	5.06	0.35	N	7.6
3621	17.053	0.932	5.17	0.72	N	12.4
3033	17.361	0.838	5.32	0.35	N	21.5
2625	17.263	0.946	5.51	0.18	N	6.8
2840	17.044	1.021	5.74	0.01	N	9.2
2915	17.252	0.933	6.87	0.60	N	17.0
3245*	17.297	0.915	7.36	0.68	Y	7.7
3573*	17.452	0.998	7.74	0.72	Y	8.9
2732*	17.335	0.938	8.37	0.72	Y	14.7
2437	17.428	0.971	10.20	-0.15	N	13.2
2627*	17.265	0.929	10.45	0.82	Y	11.9
2965*	17.369	0.901	14.48	0.77	Y	27.5

Table 4.16: Solar analogs in NGC 7789 on the yearly timescale. The stars are plotted in Figures 4.28 and 4.29. α_v is the significance index. r is the correlation coefficient, and the column "99% sig?" indicates whether or not the correlation is significant at the 99% level. All stars have seven seasons of observations in V. All stars have six seasons of observations in B, except 3621, which has five. All stars have four seasons of observations in I, except 3573 and 3621, which have three. All stars have four season of observations in R, except 3621, which has three. The last column is the activity indices through the V filter for each star. An asterisk denotes an active star.

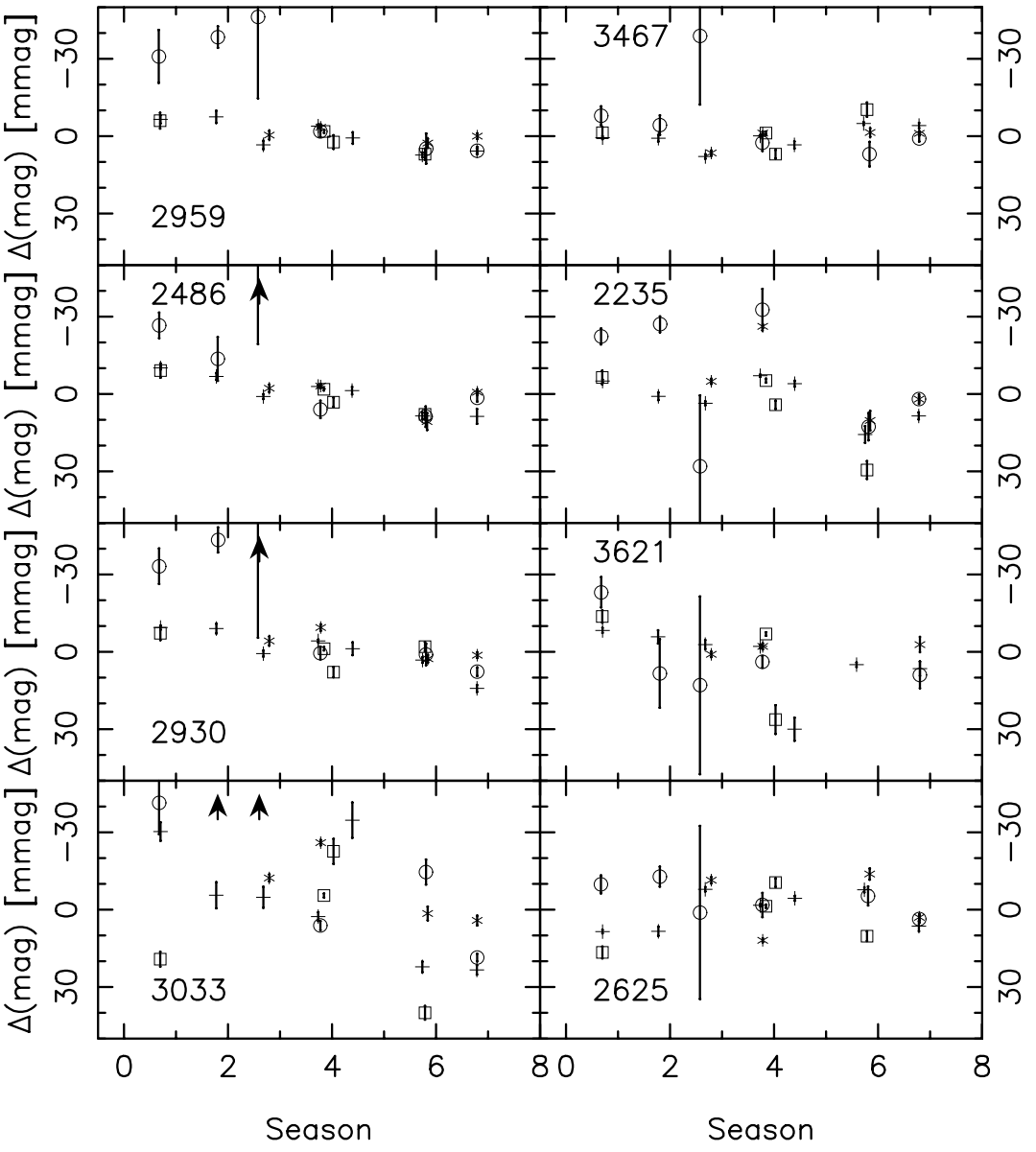

Figure 4.28: Solar analogs in NGC 7789 for individual stars on the yearly timescale. Season 0 is 1996. Stars are ordered by increasing significance index. Star properties are listed in Table 4.16. Units on y-axis are millimagnitudes. Error bars are included on all points. An arrow indicates where a point falls off the plot. Crosses are V, circles are B, boxes are I and asterisks are R. Stars are arranged in order of increasing significance index. More solar analogs are displayed in Figure 4.29.

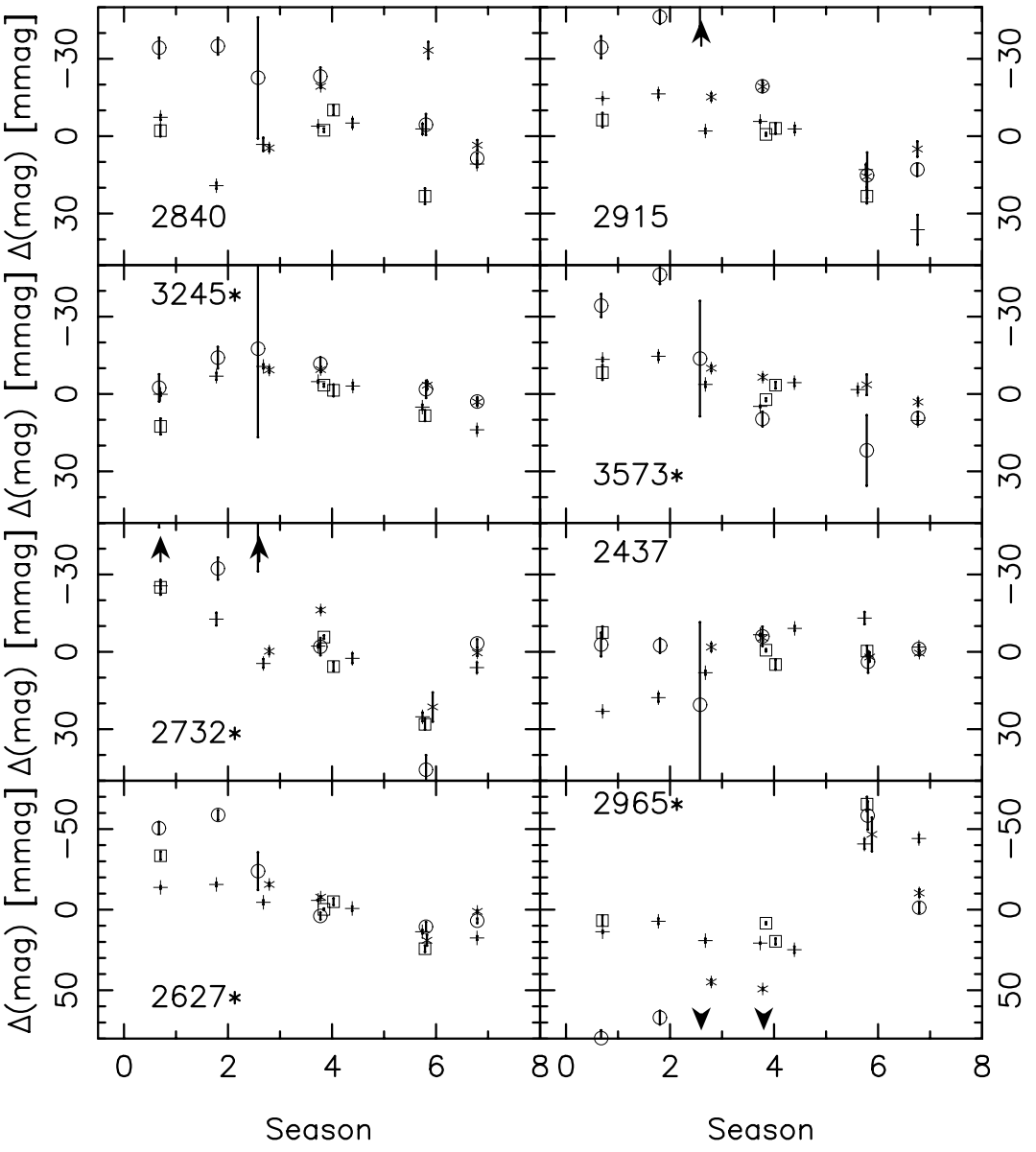

Figure 4.29: Solar analogs in NGC 7789 for individual stars on the yearly timescale, continued from Figure 4.28. Season 0 is 1996. Stars are ordered by increasing significance index. Star properties are listed in Table 4.16. Units on y-axis are millimagnitudes. Error bars are included on all points. An arrow indicates where a point falls off the plot. Crosses are V, circles are B, boxes are I and asterisks are R. Stars are arranged in order of increasing significance index. An asterisk denotes an active star.

Star	V	B-V	α_v	r	99% sig?	# R	A_v
3465	16.786	0.760	1.79	-0.10	N	4	5.2
2959	16.868	0.865	2.46	0.23	N	4	5.1
4359	16.789	0.809	3.36	0.48	N	4	11.8
3128	16.866	0.790	3.71	0.64	N	4	11.1
3380	17.089	0.881	4.29	0.55	N	2	30.1
3349	16.768	0.729	4.51	0.50	N	4	30.1
3994	16.851	0.753	5.06	0.51	N	4	26.6
3885	17.204	0.843	5.08	0.36	N	4	30.5
3605	17.217	0.820	5.10	0.54	N	4	14.8
3842	16.937	0.790	5.32	0.50	N	4	14.2
2939	16.764	0.741	5.50	0.54	N	4	18.2
3043	16.733	0.740	5.74	0.44	N	4	8.9
3691	16.962	0.792	5.92	0.36	N	4	17.9
3336	17.102	0.890	6.11	0.49	N	4	25.3
3214*	16.842	0.883	6.20	0.78	Y	4	25.4
3539	16.897	0.737	6.45	0.16	N	4	21.3
3914	16.782	0.726	6.93	0.61	N	3	19.8
4254*	17.235	0.858	7.25	0.77	Y	4	28.3
3995*	17.000	0.783	7.33	0.75	Y	4	15.7
2818	17.120	0.829	8.22	0.59	N	4	27.0
2945*	16.870	0.772	8.85	0.69	Y	4	27.3
3140*	17.041	0.791	9.21	0.71	Y	4	58.8
3500	16.913	0.794	9.36	0.47	N	4	34.7
2906	16.994	0.823	10.02	0.55	N	4	38.8
4236*	17.231	0.814	13.22	0.79	Y	2	98.8

Table 4.17: Solar analogs in NGC 6819 on the yearly timescale. The stars are plotted in Figures 4.30, 4.31, and 4.32. α_v is the significance index. r is the correlation coefficient, and the column "99% sig?" indicates whether or not the correlation is significant at the 99% level. All stars have seven seasons of observations in V and B. All stars have four seasons of observations in I. The number of seasons of observations of R is listed for each star. The last column is the activity indices through the V filters for each star. An asterisk denotes an active star.

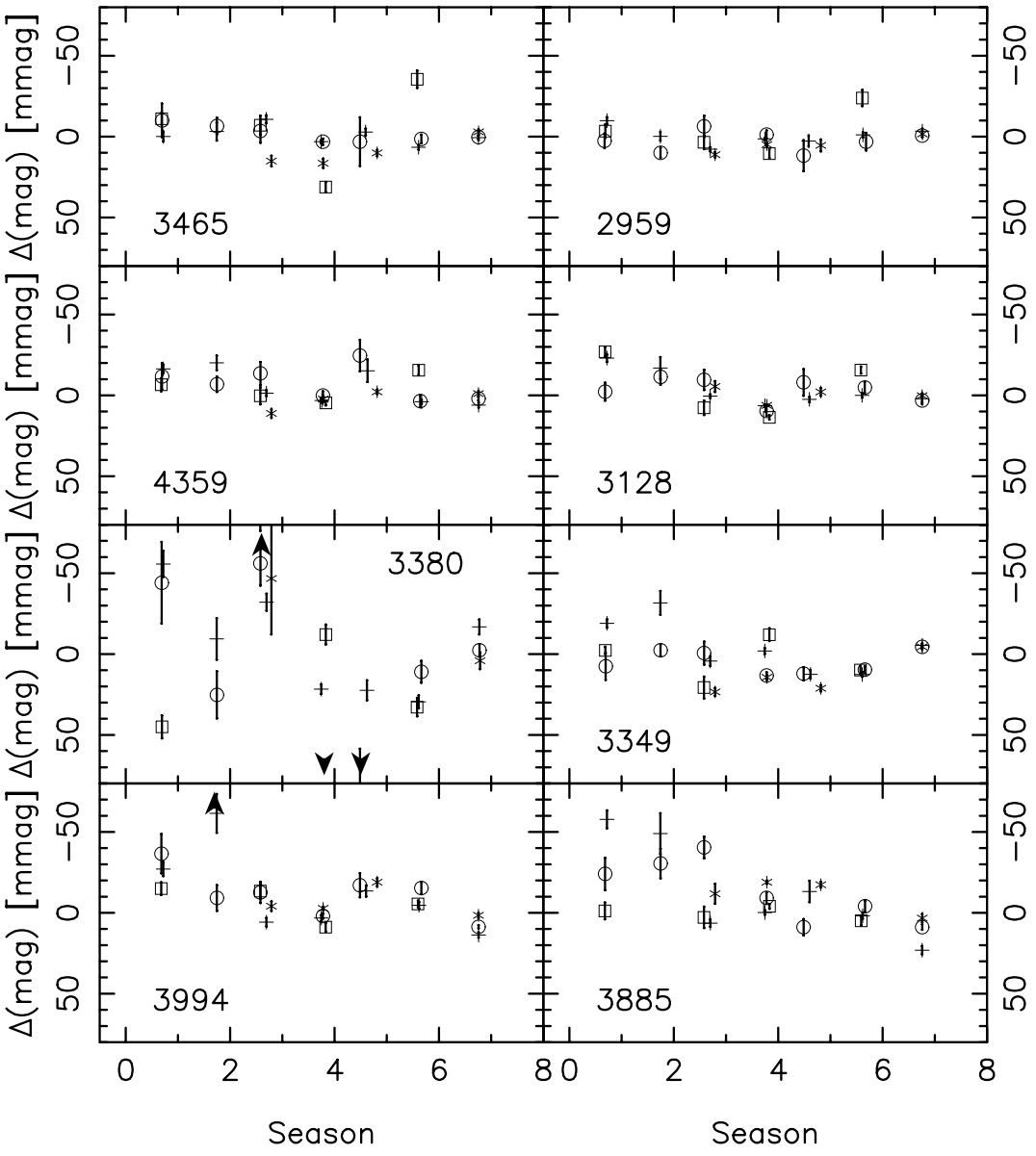

Figure 4.30: Solar analogs in NGC 6819 for individual stars on the yearly timescale. Season 0 is 1996. Star properties are listed in Table 4.17. Units on y-axis are millimagnitudes. Error bars are included on all points. An arrow indicates where a point falls off the plot. Crosses are V, circles are B, boxes are I and asterisks are R. Stars are arranged in order of increasing significance index. An asterisk denotes an active star. More solar analogs are displayed in Figures 4.31 and 4.32.

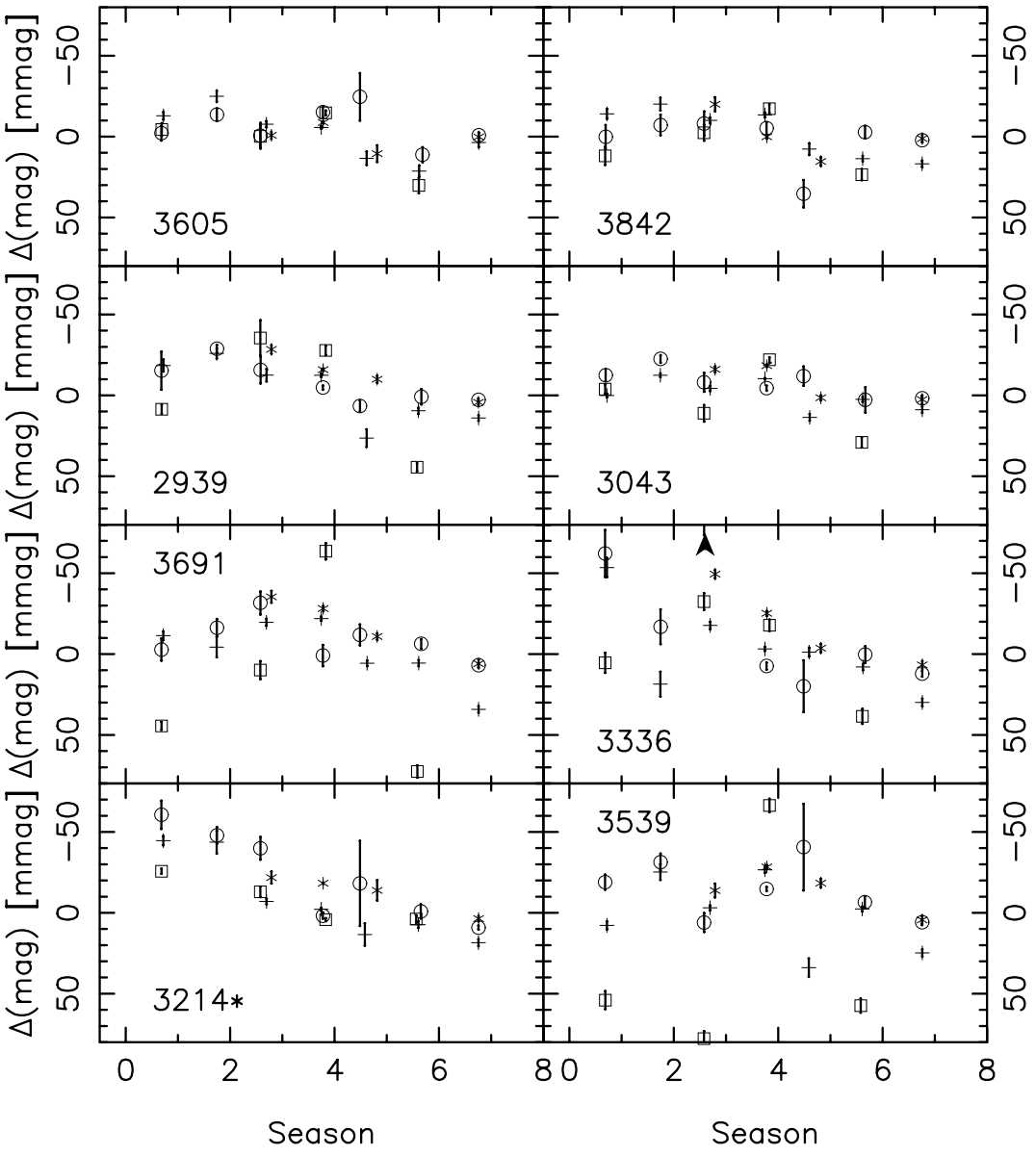

Figure 4.31: Solar analogs in NGC 6819 for individual stars on the yearly timescale. Season 0 is 1996. Star properties are listed in Table 4.17. Units on y-axis are millimagnitudes. Error bars are included on all points. An arrow indicates where a point falls off the plot. Crosses are V, circles are B, boxes are I and asterisks are R. Stars are arranged in order of increasing significance index. An asterisk denotes an active star. More solar analogs are displayed in Figures 4.30 and 4.32.

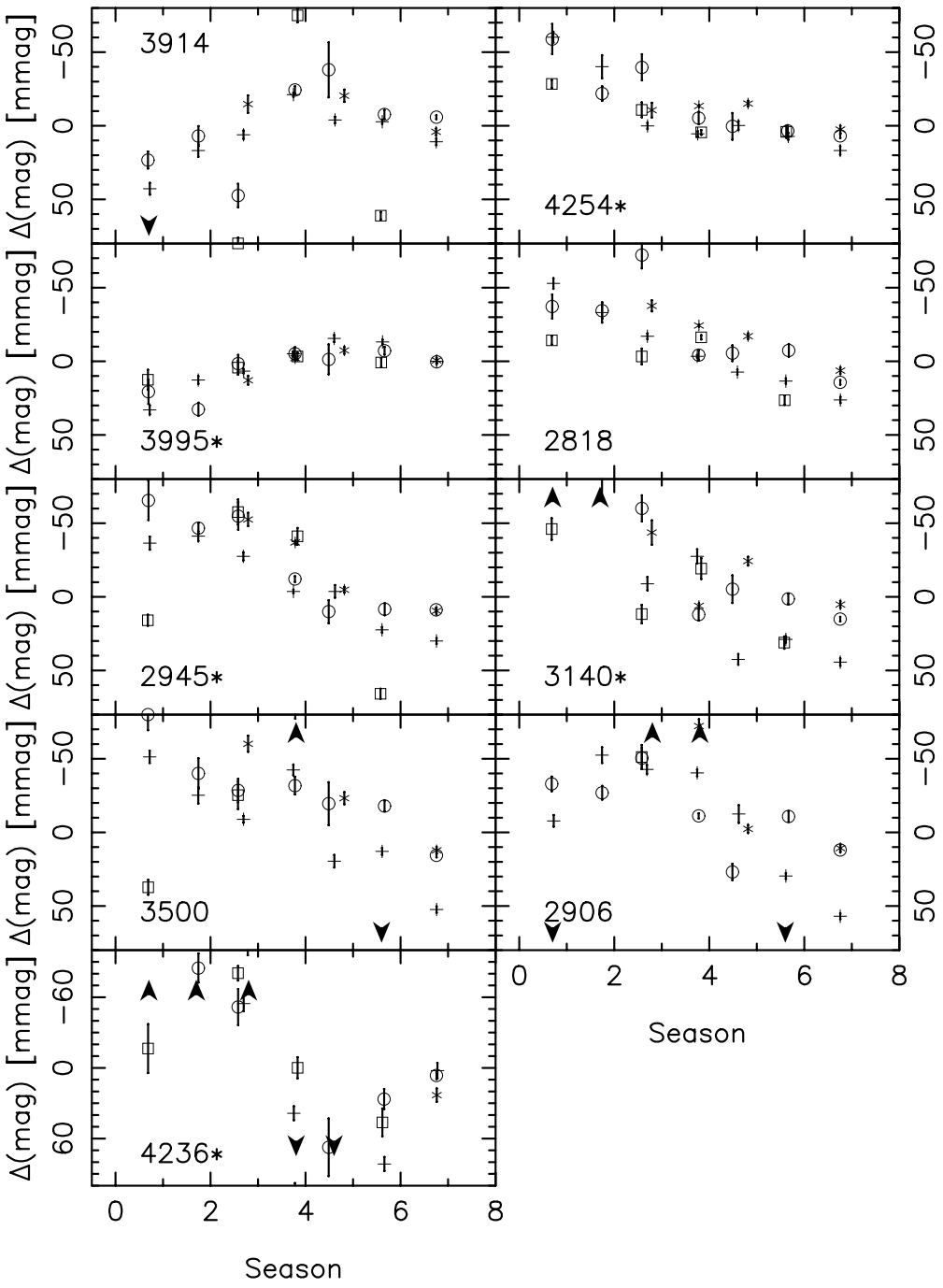

Figure 4.32: Solar analogs in NGC 6819 for individual stars on the yearly timescale. Season 0 is 1996. Star properties are listed in Table 4.17. Units on y-axis are millimagnitudes. Error bars are included on all points. An arrow indicates where a point falls off the plot. Crosses are V, circles are B, boxes are I and asterisks are R. Stars are arranged in order of increasing significance index. An asterisk denotes an active star. More solar analogs are displayed in Figures 4.30 and 4.31.

Star	V	B-V	α_v	r	99% sig?	# V	# B	# R	A_v
5709	15.214	0.793	1.52	0.78	N	7	3	5	7.6
5807	14.718	0.729	2.63	0.25	N	7	3	5	1.3
5829	14.411	0.685	3.65	0.20	N	7	3	4	1.6
5770	15.055	0.797	4.97	0.38	N	7	3	5	7.6
5768	14.928	0.759	6.46	0.33	N	8	4	6	3.4
5777	14.516	0.737	7.77	0.23	N	8	4	6	7.2
5788	14.183	0.711	8.54	0.08	N	8	4	6	8.4
5776	14.122	0.606	8.67	-0.34	N	8	4	5	10.6
5937	14.191	0.625	8.92	-0.33	N	7	3	4	8.0
5594	14.160	0.708	9.41	-0.40	N	8	4	5	9.2
5748*	14.335	0.807	35.71	0.90	Y	7	3	6	43.5

Table 4.18: Solar analogs in M67 on the yearly timescale. The stars are plotted in Figures 4.33 and 4.34. α_v is the significance index. r is the correlation coefficient, and the column " 99% sig?" indicates whether or not the correlation is significant at the 99% level. Columns 7 - 9 list the number of seasons of observations through the V, B, and R filters. All stars have two seasons of observations through the I filter. The last column lists the activity indices for each star through the V filter. An asterisk denotes an active star.

Star	V	B-V	α_v	r	99% sig?	# V	# B	# R	A_v
851	16.103	0.700	1.24	0.26	N	8	7	6	11.2
648	16.436	0.766	1.53	-0.29	N	8	7	6	2.6
709	16.059	0.821	2.32	0.73	Y	8	7	6	4.3
611	16.093	0.722	2.68	0.12	N	7	5	3	3.3
574	16.377	0.803	2.92	0.24	N	8	7	6	4.0
731	16.080	0.823	3.21	0.20	N	8	3	3	90.1
549	16.354	0.757	3.33	-0.06	N	7	5	5	3.4
577	16.090	0.720	4.54	-0.16	N	8	7	6	5.3
645	16.335	0.760	9.50	0.24	N	8	7	6	11.7

Table 4.19: Solar analogs in NGC 188 on the yearly timescale. The stars are plotted in Figure 4.35. α_v is the significance index. r is the correlation coefficient, and the column "99% sig?" indicates whether or not the correlation is significant at the 99% level. All stars have four seasons of observations in I, except 731, which has no I annual mean. Columns 7 - 9 list the number of seasons of observations in V, B, and R. The last column lists the activity indices for each star calculated through the V filter.

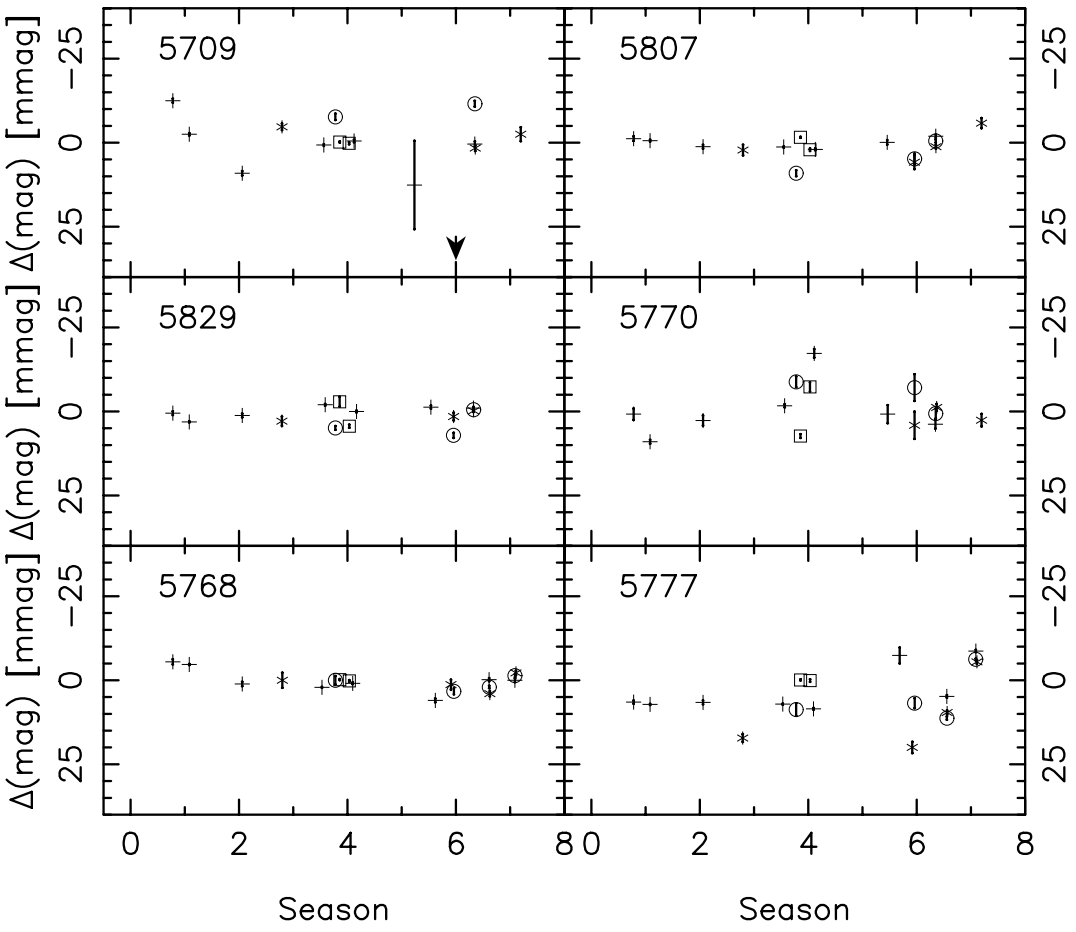

Figure 4.33: Solar analogs in M67 for individual stars on the yearly timescale. Season 0 is 1996. Star properties are listed in Table 4.18. Units on y-axis are millimagnitudes. Error bars are included on all points. An arrow indicates where a point falls off the plot. Crosses are V, circles are B, boxes are I and asterisks are R. Stars are arranged in order of increasing significance index. More solar analogs are displayed in Figure 4.34.

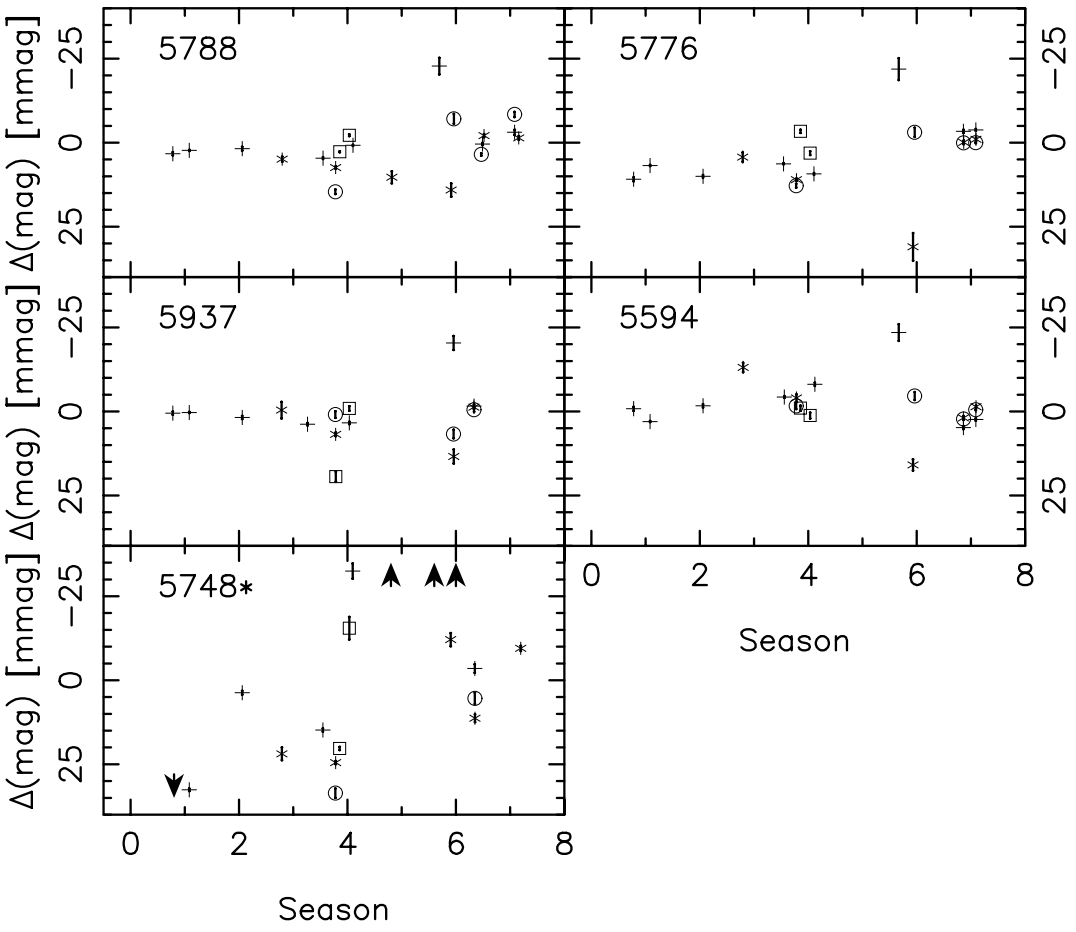

Figure 4.34: Solar analogs in M67 for individual stars on the yearly timescale. Season 0 is 1996. Star properties are listed in Table 4.18. Units on y-axis are millimagnitudes. Error bars are included on all points. An arrow indicates where a point falls off the plot. Crosses are V, circles are B, boxes are I and asterisks are R. Stars are arranged in order of increasing significance index. More solar analogs are displayed in Figure 4.33.

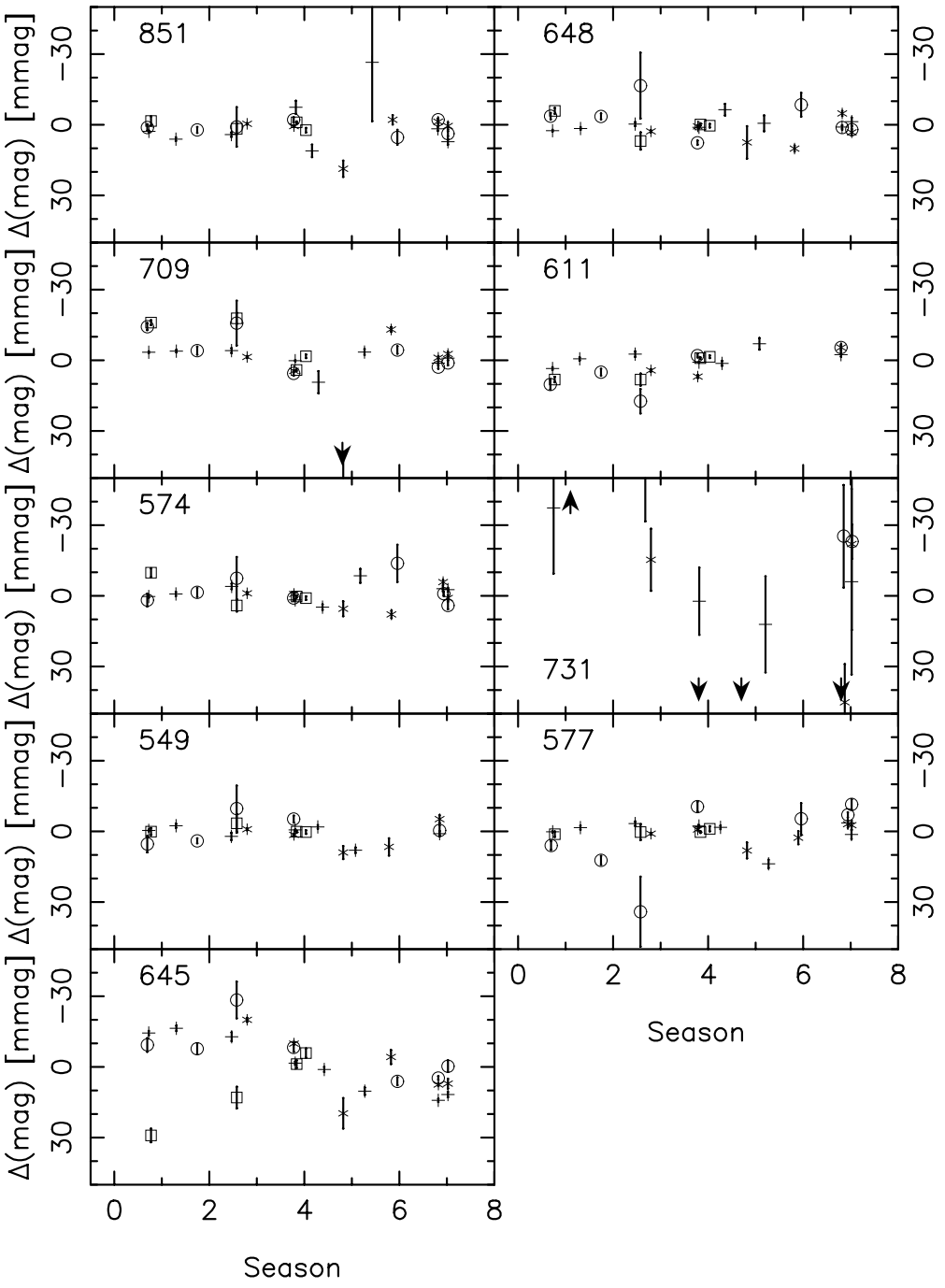

Figure 4.35: Solar analogs in NGC 188 for individual stars on the yearly timescale. Season 0 is 1996. Star properties are listed in Table 4.19. Units on y-axis are millimagnitudes. Error bars are included on all points. An arrow indicates where a point falls off the plot. Crosses are V, circles are B, boxes are I and asterisks are R. Stars are arranged in order of increasing significance index. Star 731 has no I data.